Orthogonal folding of extensional detachments: Structure and origin of the Sierra Nevada elongated dome (Betics, SE Spain)

J. M. Martínez-Martínez and J. I. Soto

Instituto Andaluz de Ciencias de la Tierra (CSIC) and Departamento de Geodinámica, Universidad de Granada, Granada, Spain

J. C. Balanyá

Departamento de Ciencias Ambientales, Facultad de Ciencias Experimentales, Universidad Pablo de Olavide, Sevilla, Spain

Received 22 January 2001; revised 23 October 2001; accepted 14 December 2001; published 25 May 2002.

[1] A close relationship of the kinematics and timing between low-angle extensional faulting and upright folding is established for the Miocene detachment systems in the hinterland of the Betics in southeastern Spain. Folding accompanied tectonic denudation developing elongated domes with fold axes both parallel and perpendicular to the direction of extension. The geometry, kinematics, and tectonic evolution of two major sequentially developed extensional fault systems have been characterized in several E-W elongated mountain ranges of the central Betics on the basis of new cartographic and structural data and a comprehensive revision of other available geological and geophysical observations. The extensional systems have an average WSW direction of extension and led to exhumation of the two lower metamorphic complexes of the Betics, the Nevado-Filabride and the Alpujarride, during the middle and upper Miocene (Serravallian to Tortonian). The extended domain contains a core complex, with distal and proximal antiformal hinges separated by around 60 km and with a fold amplitude of ∼6 km (measured parallel to the direction of extension). The total amount of extension across the core complex is about 109–116 km, corresponding to a stretching factor (β) of 3.5–3.9, estimated using the distance between fold axial surfaces and a geometrical model accomplishing footwall deformation during tectonic denudation via subvertical simple shear. The elongated domal and basinal geometry of the detachments and their respective footwalls is due to the interference between two sets of orthogonal large-scale open folds, trending N-S and E-W. Longitudinal, N-S trending folds are interpreted as isostatic folds, i.e., folds that developed in response to differential unloading of the extensional detachment footwalls inducing ductile flow in the middle crust. These folds formed in a rolling-hinge anticline in which rotation migrates westward through the footwall as it is progressively unroofed. In contrast, E-W trending folds, being subparallel to the direction of extension, have a contractional origin and progressively affect to the west the isostatically readjusted segments of the detachments once they are inactive. Orthogonal folding occurred since the Serravallian to lower Pliocene. Extension is still active from the rolling-hinge anticline in Sierra Nevada to the west. The middle Miocene to Pliocene tectonic evolution of the Sierra Nevada elongated dome at the core of the Betic hinterland is another example of the coexistence of extension and contraction during continued overall convergence and mountain-building. *INDEX TERMS:* 8109 Tectonophysics: Continental tectonics—extensional (0905); 8005 Structural Geology: Folds and folding; 8010 Structural Geology: Fractures and faults; 8025 Structural Geology: Mesoscopic fabrics; *KEYWORDS:* extensional detachments, elongated domes, orthogonal folds, unroofing, Betics, Mediterranean

0278-7407/02/2001TC001283$12.00

1. Introduction

[2] The synchronous development of low-angle normal faults (extensional detachments) and large-scale upright folds has been well documented in extended terranes throughout the world [e.g., *Spencer*, 1984; *John*, 1987; *Wernicke and Axen*, 1988; *Getty and Gromet*, 1992; *Mancktelow and Pavlis*, 1994; *Axen et al.*, 1998; *Tari et al.*, 1999; *Yin et al.*, 1999]. Moreover, doubly plunging antiformal (domal) and synformal (basinal) geometries affecting both the detachment faults and their respective footwalls have fold axes both parallel and perpendicular to the direction of extension.

[3] It is a matter of debate as to whether these folds are formed by a single process or are related to the superposition of two mechanically independent processes. The single-process models that have been proposed are (1) the emplacement of synextensional plutons [*Holt et al.*, 1986; *Reynolds and Lister*, 1990; *Amato et al.*, 1994; *Davis and Henderson*, 1999]; (2) uncompensated undulatory Moho geometry during extension [*Yin*, 1989, 1991]; and (3) horizontal compression perpendicular to the direction of extension, generating finite constrictional deformations [*Bartley et al.*, 1990; *Buick*, 1991; *Yin and Dunn*, 1992; *Chauvet and Séranne*, 1994; *Mancktelow and Pavlis*, 1994; *Kurz and Neubauer*, 1996; *Hartz and Andressen*, 1997; *Lammerer and Weger*, 1998].

[4] Other authors have concluded, in contrast, that the formation of domal and basinal detachment faults is the result of the interference between two independent processes. Folds with hinges trending perpendicular to the direction of extension have been interpreted as having been formed by (1) reverse drag caused by movement over a structurally deeper detachment [*Spencer*, 1984; *Bartley and Wernicke*, 1984; *Gans et al.*, 1985; *Davis and Lister*, 1988; *Brady et al.*, 2000]; (2) the formation of antithetic shear zones in the lower plate [*Reynolds and Lister*, 1990; *Kruger et al.*, 1998]; (3) movement along a flat-ramp fault surface, producing fault bend folding [*John*, 1987]; and (4) isostatic rebound due to tectonic denudation [*Rehrig and Reynolds*, 1980; *Spencer*, 1984;

Buck, 1988; *Wernicke and Axen*, 1988] inducing ductile flow in the lower [*Block and Royden*, 1990] or in the middle crust [*Wernicke*, 1992; *Axen et al.*, 1995]. In the latter model, it has been proposed that folds trending perpendicular to the direction of extension developed through a "rolling hinge" mechanism in which rotation migrates through the footwall as it is progressively unroofed [*Buck*, 1988; *Hamilton*, 1987; *Wernicke and Axen*, 1988; *Bartley et al.*, 1990; *Axen and Wernicke*, 1991; *Spencer and Reynolds*, 1991; *Wdowinski and Axen*, 1992; *Manning and Bartley*, 1994; *Axen et al.*, 1995; *Lee*, 1995; *Axen and Bartley*, 1997; *Lavier et al.*, 1999]. Folds parallel to the direction of extension have variously been interpreted as: (1) original fault corrugations [*Davis and Hardy*, 1981; *Spencer*, 1985; *John*, 1987; *Davis and Lister*, 1988; *Miller and John*, 1999]; (2) contractional folds of initially planar detachment faults [*Spencer*, 1984, 1985]; (3) folds due to differential uplift in a lateral ramp (analogous to the formation of hanging wall rollover folds) [*Duebendorfer and Sharp*, 1998]; and (4) folds attributed to synplutonic deformation [*Coleman et al.*, 1997; *Davis and Henderson*, 1999] or postmagmatic extensional-related collapse [*Anderson et al.*, 1994].

[5] Large-scale upright folds are a common structure in the Betics in SE Spain and have mainly determined the current physiography of the chain, which consists of a basin and range morphology with anticlines occupying the ranges and synclines in the basins. Noteworthy among the mountain ranges is the Sierra Nevada core complex [*Martínez-Martínez et al.*, 1997b], which occupies the inner part of a large-scale elongated domal structure where the lowest tectono-metamorphic nappe complex of the internal Betics is exposed. On the basis of both new structural data from the Sierra Nevada and the revision of geological data in a broader area, we have attempted to determine (1) the location of major extensional necks (highly extended zones) and the implications of their time-space changes and (2) the chronological and, if any, genetic relationships between extension and the two sets of large-scale folds, trending subparallel and subperpendicular to the direction of extension. The combined analysis of extensional fault systems and folding shows that two main extensional detachments are required to explain both the observed geometry and the distribution of the fault rocks.

2. Tectonic Setting

[6] The Betics in southern Spain form the northern branch of the peri-Alborán orogenic system (western Mediterranean), which includes the Rif and Tell mountains in North Africa. The Betics and Rif are linked across the Strait of Gibraltar to form an arcuate orogen commonly known as the Gibraltar arc (inset in Figure 1). Several pre-Miocene terrains form part of the arc: (1) the South-Iberian domain and (2) the Maghrebian domain, both consisting of nonmetamorphic Triassic to Miocene sediments deposited on the continental margins of the southern Iberian and northern African plates, respectively; (3) the Flysch Trough domain, which comprises mainly lower Cretaceous to early Miocene deep marine clastic sediments deposited in a trough between the paleomargins, along the Iberia-Africa transform boundary [*Biju-Duval et al.*, 1977; *Wildi*, 1983]; and (4) the Alborán domain, made up mainly of Paleozoic and Mesozoic rocks, mainly deformed under variable metamorphic conditions during the Cretaceous to Paleogene. This domain includes the Internal Zones of the Betics and Rif and also constitutes the thin continental basement of the Alborán basin, a Neogene extensional basin developed behind the Gibraltar arc [*Comas et al.*, 1992, 1999].

[7] The Alborán domain consists of a large number of stacked thrust sheets grouped into three nappe complexes: the Nevado-Filabrides, the Alpujarrides, and the Malaguides, in ascending order. Stacking occurred during the pre-Miocene in a more easterly position, probably when the Alborán domain was a segment of the continuous Alpine orogenic belt [*Bouillin et al.*, 1986]. The Nevado-Filabride rocks, ranging in age from Paleozoic to Cretaceous, show polyphase Alpine metamorphism with an early high-pressure/low-temperature (HP/LT) metamorphism, followed by high-greenschist facies in the two lower tectonic units and almandine-amphibolite facies in the uppermost one [*Nijhuis*, 1964; *Gómez-Pugnaire and Fernández-Soler*, 1987; *García-Dueñas et al.*, 1988; *Bakker et al.*, 1989; *Soto*, 1991]. The Alpujarride rocks, mainly consisting of Paleozoic metapelites and Triassic carbonate rocks, also show polyphase Alpine metamorphism with a first HP/LT event followed by isothermal decompression inducing metamorphism of intermediate to low pressure [*Goffé et al.*, 1989; *Tubía et al.*, 1992; *Azañón et al.*, 1997; *Balanyá et al.*, 1997]. In each Alpujarride tectonic unit the metamorphic grade increases downward in the sequence. Moreover, the upper units show a higher grade than the lower ones. This observation suggests that stacking was postmetamorphic [*Balanyá et al.*, 1997; *Azañón and Crespo-Blanc*, 2000]. The Malaguide rocks, ranging in age from Silurian to Oligocene, have not undergone significant Alpine metamorphism, although the Silurian series preserve Variscan orogenic features showing very low metamorphic grade [*Chalouan and Michard*, 1990].

[8] Neogene tectonic evolution of the peri-Alborán orogenic system is mainly constrained by two closely related facts: (1) the roughly N-S convergence between the European and African plates and (2) the westward migration of the Alborán domain. This convergence results in a broad zone of distributed deformation and seismicity in the region, resulting in a diffuse plate boundary. Kinematic reconstructions reveal continuous N-S convergence between Africa and Europe from the Late Cretaceous to the upper Miocene (9 Ma), then changing to NW-SE until the Present [*Dewey et al.*, 1989; *Mazzoli and Helman*, 1994]. Westward migration was largely responsible for the collision between the Alborán domain and the South Iberian and Maghrebian paleomargins after the partial obliteration of the Flysch Trough domain. In this Neogene collisional process, the rocks of both the Flysch Trough domain and the South Iberian and Maghrebian domains (External Zones) were extremely shortened by thin-skinned thrusting and folding, while at the same time the Alborán domain underwent considerable thinning with the development of extensional detachments and associated low-angle normal faults. The Alpujarride/Nevado-Filabride boundary, traditionally considered to be a thrust, has been interpreted as one of these extensional detachments on the basis of numerous evidence, including the following:

1. The detachment staircase geometry shows flats and ramps cutting across and down toward the west through the thrust stack [*García-Dueñas and Martínez-Martínez*, 1988].
2. There is a westward sense of hanging wall displacement.
3. There is an extensional geometry of the detachment hanging wall. It is composed of tilted blocks bounded by listric normal faults coalescing on the detachment and highly extended riders [*Martínez-Martínez and Azañón*, 1997].

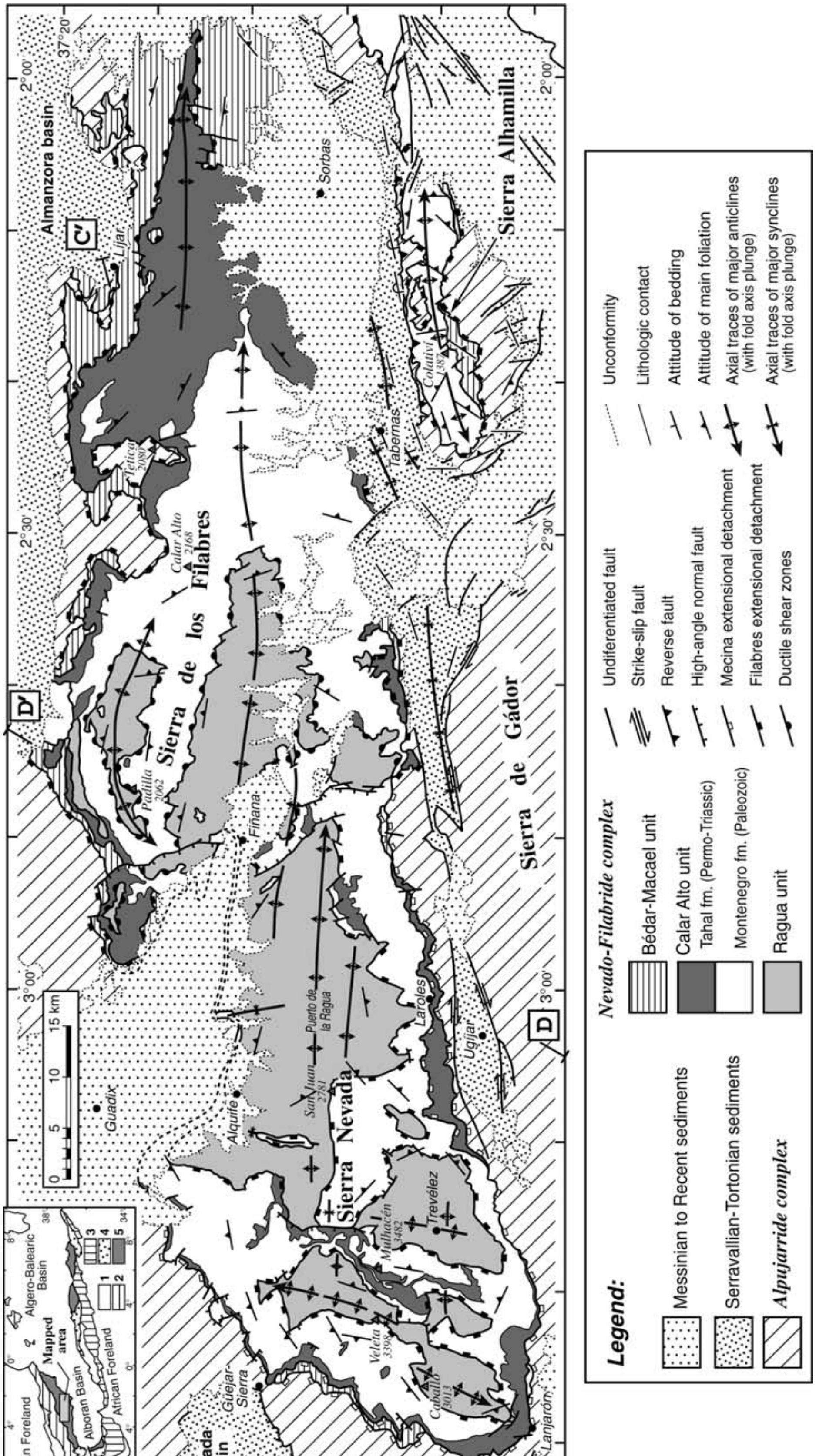

Figure 1. Tectonic map of the Sierra Nevada elongated dome (central Betics). Upper left inset shows the main tectonic domains of the peri-Alborán orogenic system: 1, Neogene basins; 2, South Iberian domain; 3, Maghrebian domain; 4, Flysch Trough units; 5, Alborán domain. Cross sections C-C′ and D-D′ are shown in Figures 6 and 11, respectively.

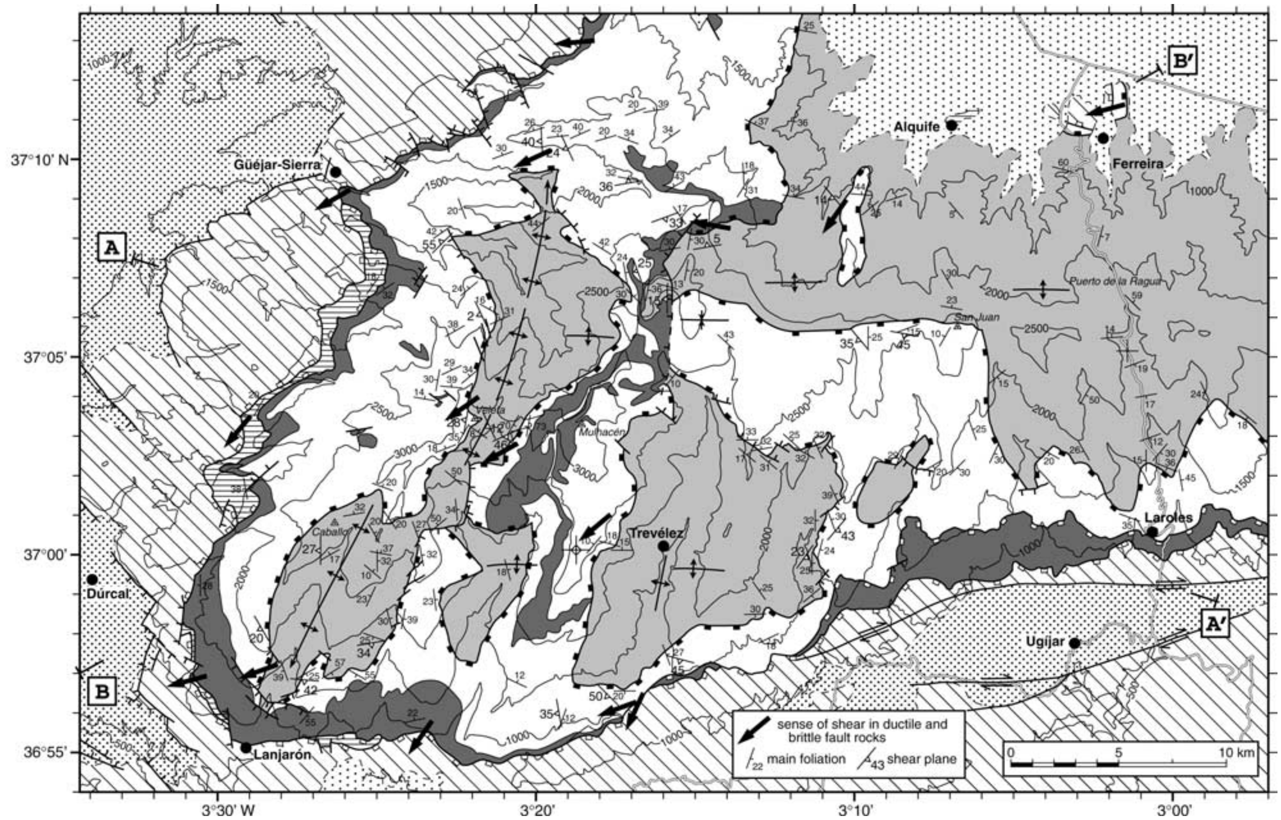

Figure 2. Structural map of the central and western Sierra Nevada. Same symbols as in Figure 1. Cross sections A–A′ and B–B′ are shown in Figure 3.

4. Local estimates for extension values for this contact are high [*García-Dueñas et al.*, 1992; *Crespo-Blanc*, 1995; *Martínez-Martínez and Azañón*, 1997].

5. The nature of fault rocks associated with the detachment is such that beneath it there are mylonites with platy foliation and penetrative stretching lineation [*Platt et al.*, 1984]. The sense of shear deduced from the lineation orientation together with kinematic indicators including S-C fabrics, rotated porphyroclasts, mica fish, and quartz C-axis fabrics are broadly consistent with a top to the west sense of shear [*Galindo-Zaldívar et al.*, 1989]. Brittle deformation produced cataclasites, fault gouges, and tectonic breccias at the Alpujarride/Nevado-Filabride contact and postdate the mylonitic deformation. This brittle deformation exhibits a sense of shear similar to that of the earlier ductile deformation, based on asymmetric textures and slickenline orientation in fault rocks [*García-Dueñas et al.*, 1988; *Galindo-Zaldívar et al.*, 1989; *Galindo-Zaldívar*, 1993; *Jabaloy et al.*, 1993].

6. Asymmetric footwall unroofing exists across the system. Cooling ages to near-surface temperatures in the footwall become younger in the direction of hanging wall motion, from 12 Ma in the eastern Sierra de los Filabres to 9 Ma in the western Sierra Nevada [*Johnson et al.*, 1997]. On the other hand, available Ar-Ar cooling ages from the upper plate are systematically older (19–24 Ma) than the corresponding ones from the lower plate (16–17 Ma) [*Monié et al.*, 1991].

[9] Extensional detachments, nonetheless, are not the most recent structures in the Alborán domain. There is well-documented evidence of large-scale E-W open folds, warping the extensional detachments [*García-Dueñas et al.*, 1986], particularly east of the Granada basin (Figure 1). Finally, high-angle normal faults and strike-slip faults, many of which are still active, offset folds and extensional detachments. High-angle normal faults are particularly abundant in western Sierra Nevada and in the Granada basin, and in a narrow, NW-SE trending band between the western Sierra de los Filabres and western Sierra Alhamilla. Strike-slip faults are more frequent in the southeastern Betics.

[10] Several tectonic models have been proposed to account for the extension of the Alborán domain within a context of plate convergence, including (1) extensional collapse driven by convective removal of the lithosphere mantle [*Platt and Vissers*, 1989], (2) delamination of the lithosphere mantle in conjunction with asymmetric thickening of the lithosphere [*García-Dueñas et al.*, 1992; *Docherty and Banda*, 1995], and (3) rapid rollback of a subduction zone [*Royden*, 1993; *Lonergan and White*, 1997], among others. However, these models do not provide a satisfactory explanation for the formation of the large-scale E-W open folds and for the recent evolution of the orogen.

3. Multiple Sets of Extensional Detachments

[11] As mentioned in section 2, the Alpujarride/Nevado-Filabride boundary, cropping out in the Sierra de los Filabres and Sierra Nevada, has been interpreted as a W-SW directed extensional detachment with associated listric normal faults [*García-Dueñas and Martínez-Martínez*, 1988; *Galindo-Zaldívar et al.*, 1989]. The detachment geometry and the nature of the associated fault rocks,

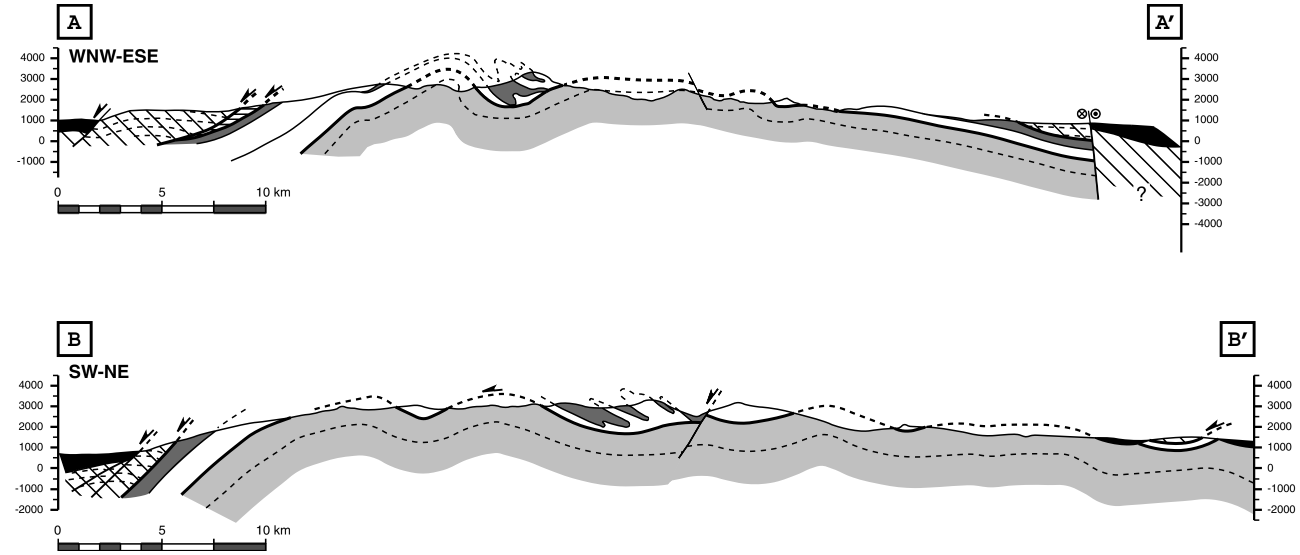

Figure 3. Structural cross sections showing the three-dimensional geometry of the Sierra Nevada elongated dome in the western sector of this mountain range. Same symbols as in Figure 1.

nevertheless, are different in the two ranges. In the Sierra de los Filabres the detachment (Filabres detachment) [*García-Dueñas et al.*, 1988; *Martínez-Martínez and Azañón*, 1997] has a low-angle footwall ramp geometry cutting 5 km of the Nevado-Filabride stack downsection in a westward direction. This footwall ramp can be observed in the map of Figure 1, where the Alpujarrides (upper plate) progressively overlie toward the west the uppermost Nevado-Filabride unit (Bédar-Macael unit) around Líjar, the Paleozoic/Permo-Triassic boundary of the intermediate Nevado-Filabride unit (Calar Alto unit) in the Tetica area, and finally, north of Fiñana, they are very close to the top of the Ragua unit, the lowermost Nevado-Filabride unit. In the Sierra de los Filabres, large-scale wedges thinning westward are defined in the footwall between the detachment and the eastward dipping regional reference surfaces, which include two large-scale ductile shear zones (500 m thick) subparallel to both the main foliation and the lithological contacts. The boundaries between the three major Nevado-Filabride units lie within these shear zones, which are synmetamorphic, and they are characterized by moderate-temperature (450°–550°C) mylonites exhibiting ESE-WNW stretching lineation and penetrative foliation associated with recrystallization and grain-growth microstructures [*Bouchez and Pêcher*, 1981]. Kinematic indicators show top to the WNW sense of shear [*Soto et al.*, 1990; *González-Casado et al.*, 1995]. In contrast, deformation related to the Filabres detachment is brittle, producing cataclasites, fault gouges, and tectonic breccias. On the other hand, the largest segment of the Alpujarride/Nevado-Filabride contact cropping out in the western Sierra Nevada (termed the Mecina detachment by *Galindo-Zaldívar et al.* [1989]) shows a footwall flat and a hanging wall ramp geometry. Cataclasites, fault gouges, and tectonic breccias are the fault rocks associated to the detachment. In the footwall there are low-temperature (350°C) mylonites and ultramylonites with a penetrative NE-SW trending stretching lineation that becomes increasingly pronounced toward the contact with the overlying Alpujarrides.

[12] The Filabres and Mecina detachments, since they coincide with the Alpujarride/Nevado-Filabride contact, have been interpreted as the eastern and western sections of the same detachment, respectively [*García-Dueñas et al.*, 1992; *Jabaloy et al.*, 1993]. Nevertheless, the structural position of the detachment in the western Sierra de los Filabres, near the top of the Ragua unit, and in the western Sierra Nevada, overlying the Bédar-Macael unit, is inconsistent with the interpretation of a unique W-SW directed extensional detachment. New cartographic and structural data carried out in the Sierra Nevada have allowed us to resolve this contradiction (Figures 2 and 3). One of the most noteworthy points is that the lowest Nevado-Filabride unit, the so-called Veleta unit [*Díaz de Federico et al.*, 1979], is less extensive than is shown in previous maps [see, e.g., *Jabaloy et al.*, 1993]. Even the Veleta peak (3398 m), after which the unit is named, is capped by Calar Alto unit rocks. In this work we have therefore changed the name of the lower unit to the Ragua, after the Puerto de la Ragua region where it is very well represented (Figure 2).

[13] Two different structural domains can be defined in the Sierra Nevada area, the western domain comprising the region located west of the Guadix-Trevélez line and the eastern domain comprising the region between this line and Fiñana village (Figure 1). In the western domain beneath the Mecina detachment, the Calar Alto unit is 3.5 km thick, which is nearly as thick as in the Sierra de los Filabres area. Internally, this unit is marked by folds with axial planes parallel to the schistosity, which developed significant reverse limbs consisting of Permo-Triassic light-colored schist (Tahal formation) below Paleozoic graphite-rich mica-schist (Montenegro formation). These folds are crosscut by the Calar Alto-Ragua boundary (Figure 3). Throughout the western Sierra Nevada the Tahal formation of the Calar Alto unit conformably overlies the Montenegro formation in a normal sequence.

[14] Mylonitic deformation (Figure 4) developed in the Mecina detachment footwall in a band ~100 m thick, affecting the entire Bédar-Macael unit and the top of the Permo-Triassic rocks of the Calar Alto unit. The Ragua/Calar Alto contact is a brittle shear zone (decimetric to metric), associated with cataclasites and fault gouges. Striations in the fault rocks trend NE-SW. Overlying the contact, a band of rocks several hundred meters thick is systematically affected by shear bands and extensional crenulation cleavage that

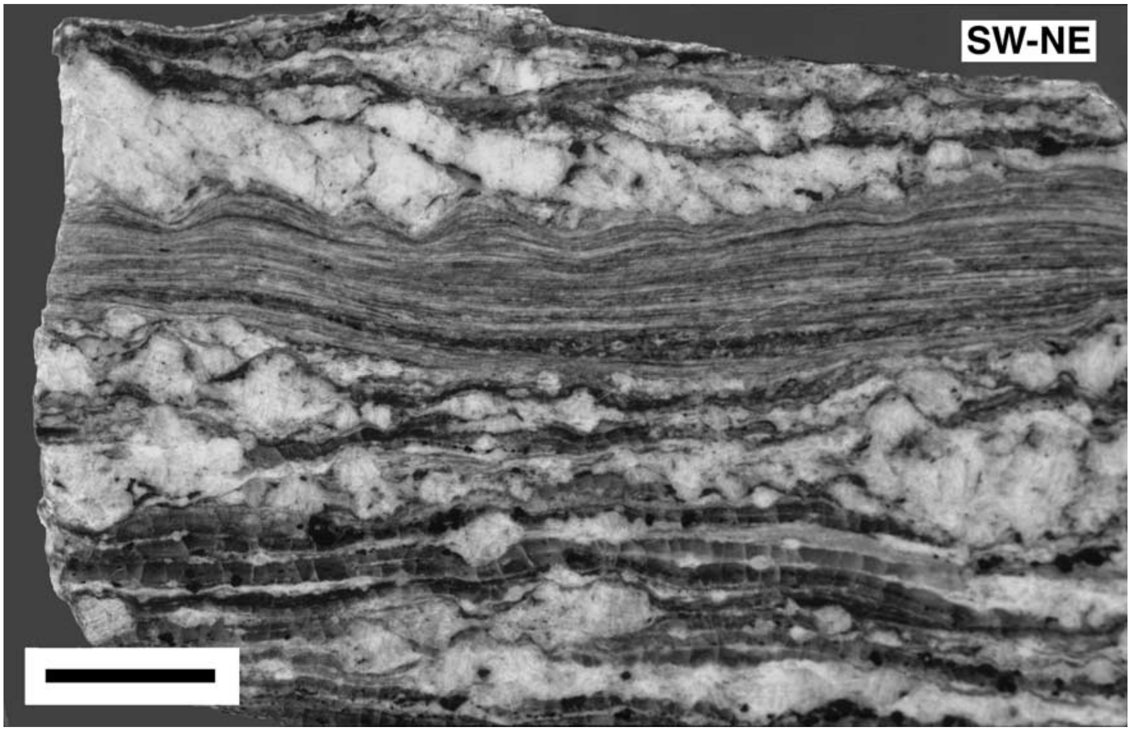

Figure 4. Footwall mylonitic gneiss of the Mecina extensional detachment showing ultramylonitic bands in a section parallel to the stretching lineation. The sense of shear is top to the left. Scale bar corresponds to 1 cm.

are more penetrative near the contact. The asymmetry of the shear bands is consistent with top to the SW sense of shear (Figure 5). In this domain, the Ragua/Calar Alto contact shows a footwall flat and low-angle hanging wall ramp geometry (Figure 3).

[15] In the eastern domain, both the Alpujarride complex and the Bédar-Macael and Calar Alto units become strongly attenuated to a few hundred or even a few tens of meters. Attenuation is evident in Figures 2 and 3 on the northern slope of the Sierra Nevada. On the

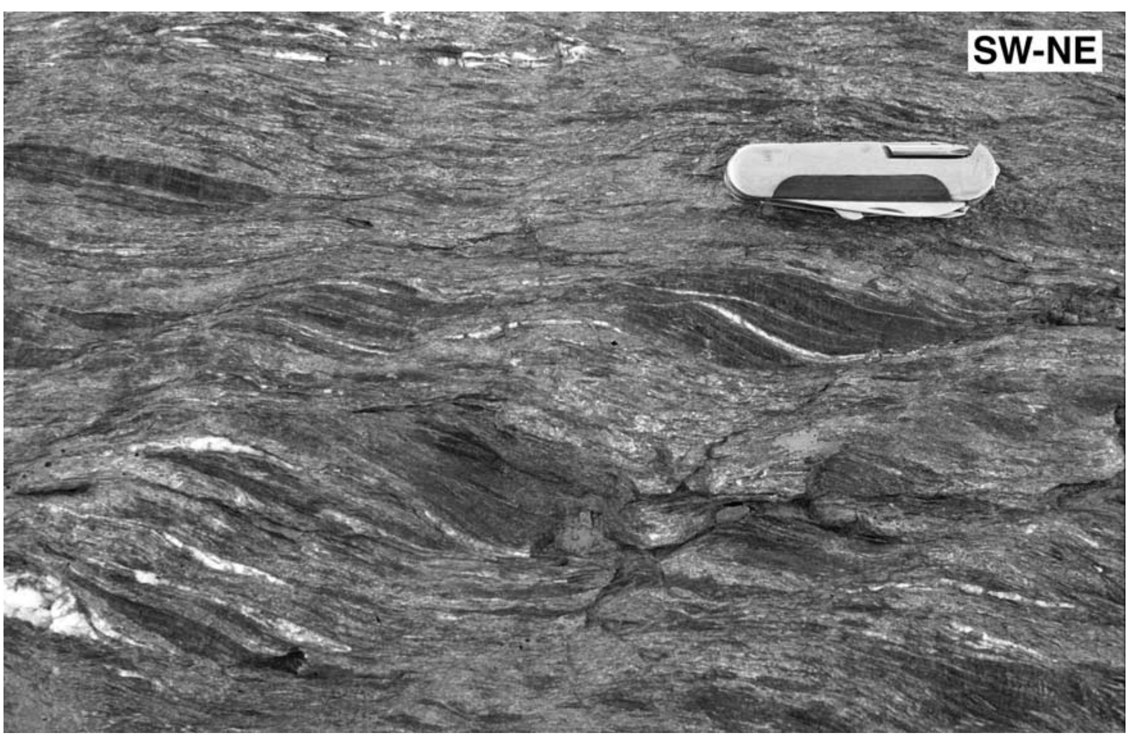

Figure 5. Ductile shear bands associated with the Filabres extensional detachment. The sense of shear is top to the left.

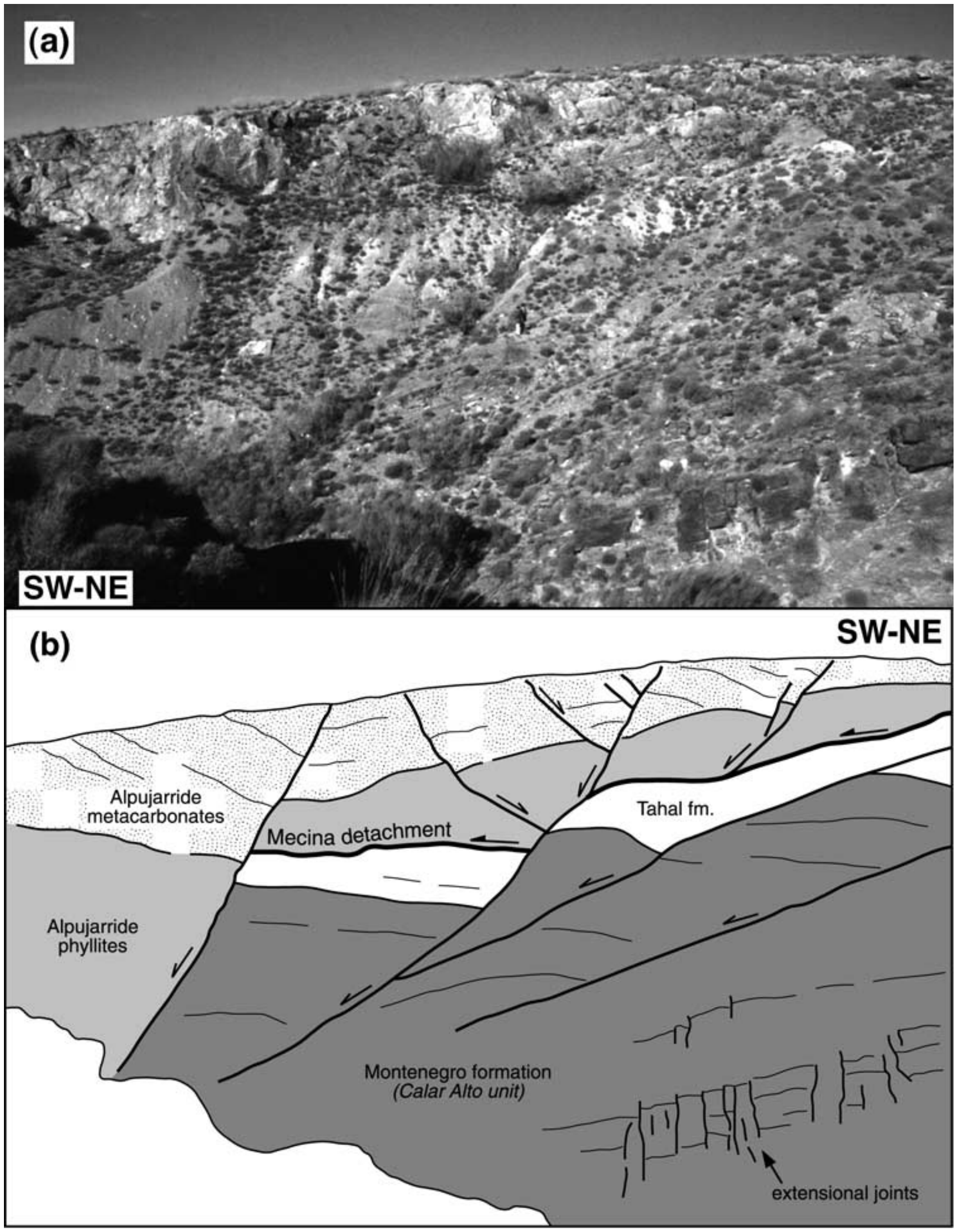

Figure 6. (a) Panoramic view and (b) drawing of the splay faults in the Filabres detachment hanging wall cutting the Mecina detachment, north of Fiñana village (see Figure 1). The Filabres detachment is a few meters below the section. There are two persons at the center of the photograph for scale.

southern slope, the Calar Alto unit, although thin (around 200 m), crops out extensively because of the fact that the contacts bounding on it dip southward at nearly the same degree as the topographic incline. In this area the Alpujarrides are also thinned (<200 m thick), particularly north of the Ugíjar basin. Further south, in the Sierra de Gádor, the Alpujarride units are thicker; however, this range belongs to a block that is structurally different from the Sierra Nevada, as they are separated by a right-handed strike-slip fault zone known as the Alpujarras strike-slip corridor [*Sanz de Galdeano et al.*, 1985]. Both the geometry of the Ragua/Calar Alto contact and the fault rocks associated with it are similar to those described in the western domain. It has a footwall flat geometry and a gently variable dip with a subhorizontal envelope. In the hanging wall there are listric fans and highly extended riders consisting of very attenuated Alpujarride, Bédar-Macael, and Calar Alto units tilted toward the east. In these riders, fragments of the Mecina detachment are cut by hanging wall splays of the Ragua/Calar Alto contact (Figure 6). This contact is connected toward the east with the Filabres extensional detachment.

[16] Altogether, this suggests that the so-called Filabres detachment is, in fact, a second detachment that developed in the footwall of the Mecina detachment. A cross section trending close to the direction of extension, from the western Sierra Nevada to the eastern Sierra de los Filabres, shows the large-scale geometry of the extensional system (section C-C′; Figure 7). The section exhibits an upward arched structure with a relatively uplifted,

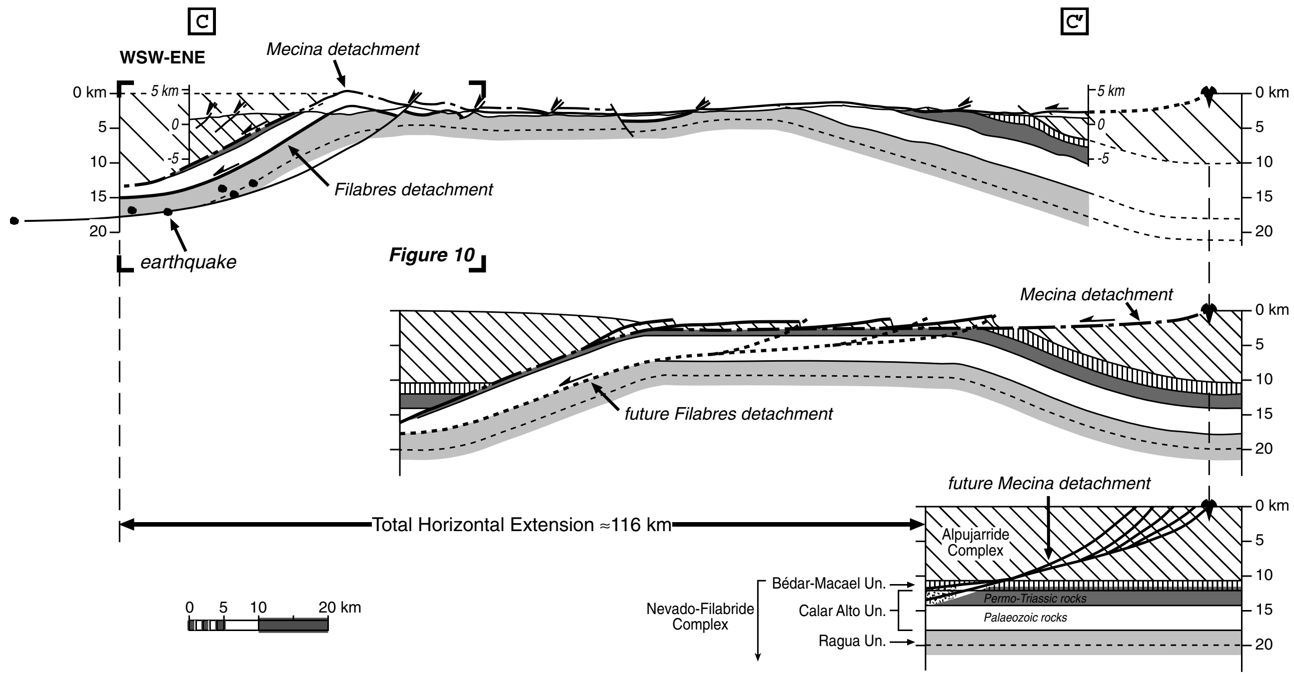

Figure 7. Structural cross section along the Sierra Nevada elongated dome, parallel to the main direction of extension. See location in Figure 1. A tentative, sequential restoration of the Mecina and Filabres detachments to the undeformed stage is also shown. Calculation details of the amount of extension are in Appendix A. Ductile deformation associated to the Mecina detachment in the unextended situation is shown by a stippled area.

highly extended central domain between two flexured, less extended eastern and western marginal domains, where major rock wedges thicken in opposite senses. These marginal domains must correspond to the proximal and distal blocks of the Filabres extensional detachment, respectively. In the distal block (western Sierra Nevada), the Mecina and Filabres detachments are separated by more than 3.5 km of unextended Nevado-Filabride rocks. In the central domain the two detachments are very closed, with the Mecina detachment cut and fragmented by hanging wall splays of the Filabres detachment (Figure 6). Finally, in the proximal block, the Filabres detachment cuts the Nevado-Filabride units downsection. The boundaries of these units, two ductile shear zones prior to the detachment, are tilted toward the east.

4. Amount of Extension

[17] A sequentially restored cross section parallel to the direction of extension illustrates the prominent characteristics of extensional fault kinematics in the extended domain (Figure 7). The restoration considers the geometric and kinematics facts described in the section above, including the thickness of the Alpujarride and Nevado-Filabride sequences in the less extended domains, the dimension and location of highly extended zones, and the distribution of mylonites and related fault rocks. The preextensional Nevado-Filabride thickness is deduced from the footwall of the Filabres detachment low-angle footwall ramp. A minimum thickness of 10 km has been assumed for the Alpujarride complex, taking into account its thickness in the less extended blocks and the load necessary to generate low-temperature mylonites directly below the Mecina detachment. Several hanging wall and footwall cutoff lines belonging to both detachments have also been detected (Figure 8a). All the cases represent the site where the detachment cuts the selected reference surfaces (e.g., the Tahal/Montenegro boundary) for the first time (from east to west). Westward of each represented "cutoff line," extensional horses developed in the highly extended central domain (striped zone in Figure 8b) giving rise to slices of the Bédar-Macael unit and of the Tahal and Montenegro formations of the Calar Alto unit. We have also included the location of the earthquake hypocenters along the section [*Serrano et al.*, 1996 and *Morales et al.*, 1997].

[18] The extended domain contains a core complex, with distal and proximal antiformal hinges separated by around 60 km and with fold amplitude of ~6 km. A first detachment (the Mecina detachment) exhumed the Alpujarride complex and the top of the Nevado-Filabride complex. The formation of a second detachment (the Filabres detachment) must be considered to account for the exhumation of the middle and lower Nevado-Filabride units; it cut back toward the footwall as extension proceeded as a result of footwall unloading. Both the distributions of the earthquake hypocenters and the focal mechanisms [*Serrano et al.*, 1996; *Galindo-Zaldívar et al.*, 1999] suggest that a third detachment is currently active below the distal block of the Filabres detachment. Pliocene to Recent high-angle normal faults, which are very common in the western Sierra Nevada and the Granada basin (Figure 7), could be related to the third detachment.

[19] The theoretical basis and details of the application to reconstruct the amount of extension in the Sierra Nevada core complex are given in Appendix A. The geometrical relationships presented there and the horizontal distance (measured parallel to the regional direction of extension) between the distal antiform and the proximal synform hinges were applied to obtain a extension of 109–116 km, corresponding to a stretching factor (β) of around

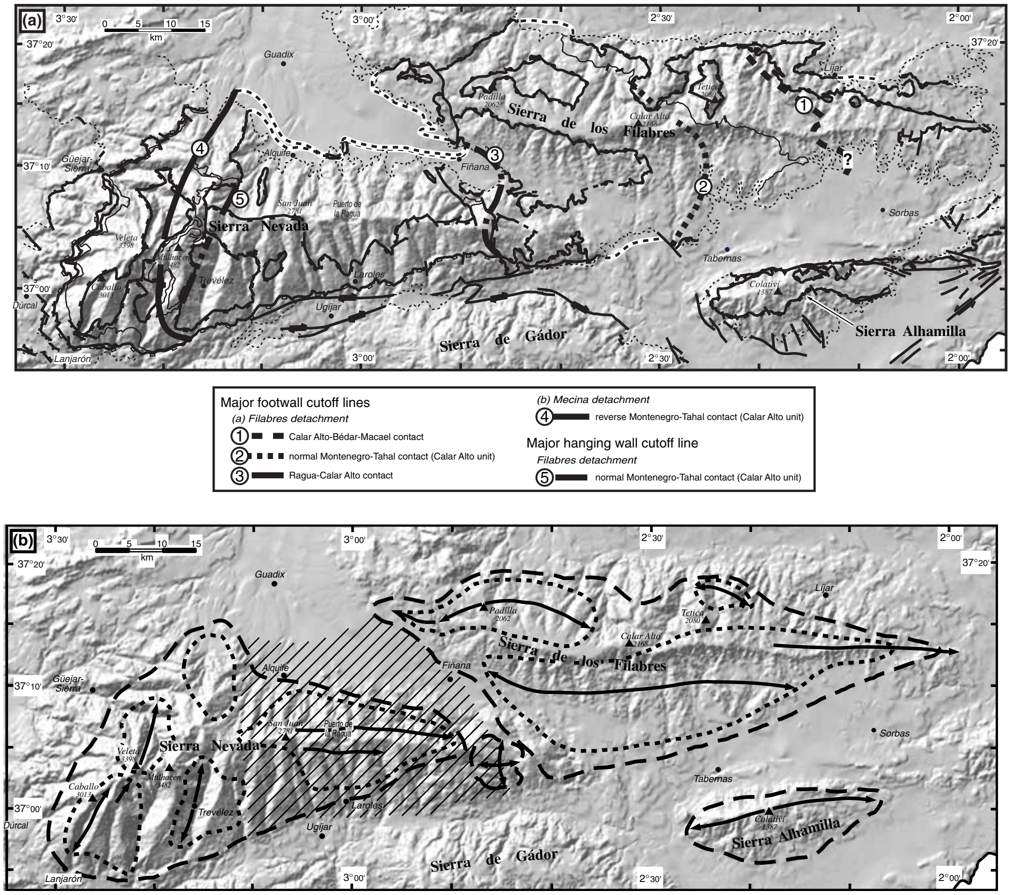

Figure 8. (a) Digital topography of the Sierra Nevada elongated dome with the extensional detachments and other main contacts, simplified from Figure 1, and the position of the major cutoff lines of the Mecina and Filabres detachments. The Filabres footwall cutoff line for the Ragua-Calar Alto contact represents the line where the hanging wall of this detachment occurs more close to this contact. (b) Tectonic sketch of the same region showing the location of the first- and second-order elongated domes. Dashed and dotted lines mark the approximate limits of domains with an outward facing dip. Striped band corresponds to the highly extended area between the proximal and distal blocks (where the maximum thickness of the Calar Alto unit is $\leq$200 m). The digital elevation data set has a horizontal grid spacing of 100 m; the vertical units represent elevation in meters above the mean sea level in Alicante (vertical exaggeration $\times$ 2). The elevation values range from 3468 to 0 meters. The digital elevation topography has been illuminated from the NW (315° azimuth and 45° of altitude or zenith distance).

3.5–3.9. It should noted that the initial situation in the undeformed stage of the reconstruction has been considered without significant topographic elevation. This interpretation is in accordance with data from regional geology, according to which the Alpujarride complex would have been the basement of a shallow marine basin during the Burdigalian-lower Langhian [*García-Dueñas et al.*, 1992]. If this were indeed the case, there has been uplift of the distal and proximal blocks as well as of the widely extended domain, especially the distal hinge anticline and the rest of the distal zone of the system (around 3 km).

5. Geometry of the Elongated Domes

[20] The contacts between the formations studied, as well as the orientation and traces of the main foliation, define elongated domes and basins. These structures have been produced, depending on the sector, either by the interference of two trends of large-scale open folds (approximately E-W and N-S, respectively) or by noncylindrical folds that die out rapidly along the fold hinge.

[21] The Nevado-Filabride outcrops between 2°W and 3°30 W (Figures 1 and 8b) largely show a structure of E-W elongated domes of different order, with a ratio between the longitudinal and transverse fold wavelength of 1.5 to 3. Two first-order domes are recognized: the Sierra Nevada and Sierra de los Filabres, separated by the Fiñana syncline. The former corresponds very closely to the main relief of the Sierra Nevada in both areal extent and three-dimensional geometry, whereas the latter includes not only the Sierra de los Filabres but also a sector south of this mountain chain (Figure 8b). Also worth noting is the double plunging anticline of the Sierra Alhamilla, connected to the elongated dome of the Sierra de los Filabres by a set of N70°–80°E folds that affect Serravallian to Tortonian sediments (Figures 1 and 8a).

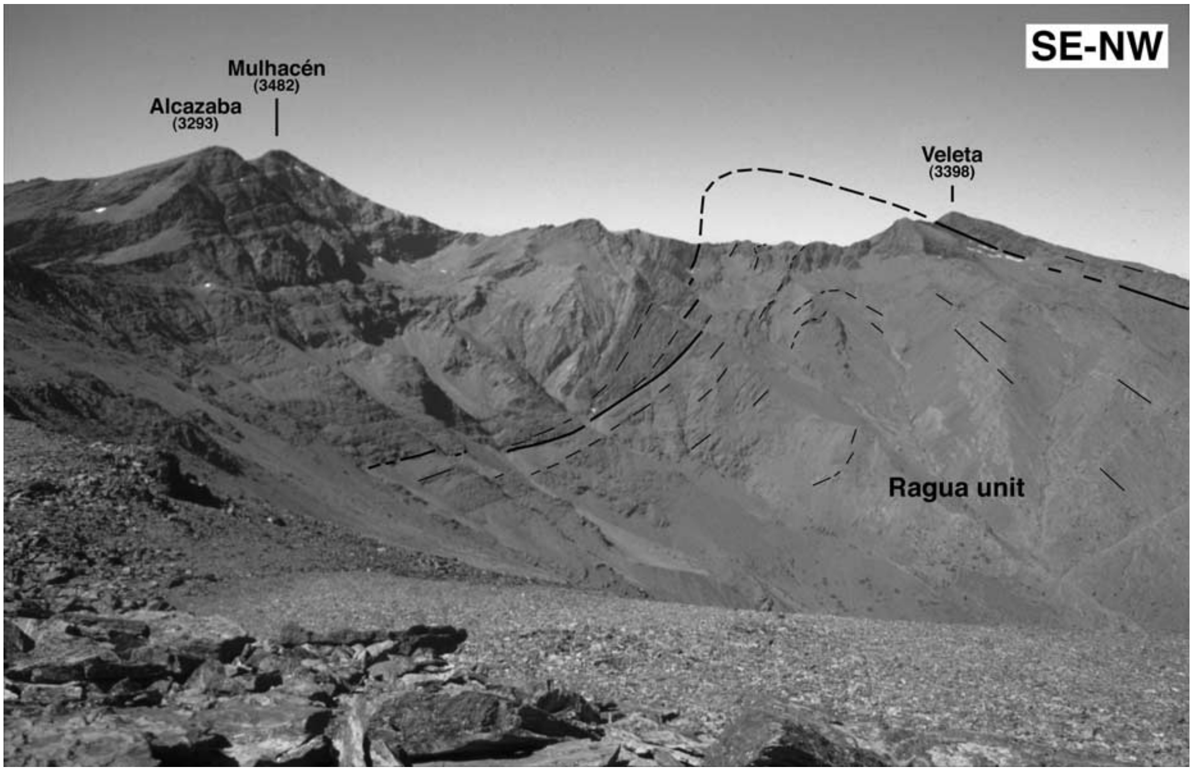

Figure 9. Landscape view (looking southwest) of the fold interference between the rolling hinge and the E-W anticlines at the highest elevations of the Sierra Nevada mountain range. The NW dip of the foliation around the Veleta peak corresponds to the western periclinal closure of the Sierra Nevada elongated dome. Note the light-colored band of crumbly brittle fault rocks associated with the Filabres detachment (thicker lines) and its hanging wall-ramp geometry.

[22] In the Filabres dome, two domains can be distinguished:

1. The eastern domain has two E-W, double-plunging antiforms that are upright or box-shaped. Associated reverse faults (in places resulting in map-scale lithostratigraphic duplications) and subhorizontal tension joints commonly develop. The hinge lines of the two antiforms form an en echelon pattern. The western end of this domain gives way to the Fiñana plunging syncline, partially hidden by Pliocene sediments (Figure 1).

2. The western domain of the Filabres dome coincides with a large doubly plunging antiform with an arcuate axial surface trace. This fold is asymmetric in cross section and is characterized by a subvertical northern flank associated with reverse faults with consistent vergence. To the west, this antiform becomes more rounded and the interlimb angle increases, suggesting that the fold dies out to the west.

[23] The Sierra Nevada dome (Figures 2 and 8) is 70 × 30 km (on a horizontal plane at an elevation of 1400 m) and comprises two parts with somewhat different characteristics. The eastern sector has the overall geometry of a north vergent antiform plunging gently eastward. Within the antiform can be found several second-order en echelon folds trending N100°E. Moreover, there are other, smaller, N-S folds of limited extent (synclines SW and east of Alquife; Figure 2). The western sector has various moderately elongated second-order domes aligned N-S to NNE-SSW whose main axis roughly converges with the culmination zone of the principal dome of Sierra Nevada (Figures 2 and 8). In this zone, coinciding with the area of highest relief (Caballo-Mulhacén crest), the profile of the main fold reaches it greatest size (half wavelength is 30 km; fold amplitude is 6 km; both values refer to the Mecina detachment; Figures 2 and 9). At its western closure, the Sierra Nevada dome plunges 15°–20°. This fold dies out rapidly toward the west, as evidenced by the unfolded Alpujarride units and Neogene sediments.

6. Discussion

[24] We discuss our results from several viewpoints. Although we have several lines of evidence to support a continuous folding event, progressing in time from folding linked to tectonic denudation along the Mecina and Filabres extensional detachments, to younger folding under N-S contraction, we will separate the arguments to discuss the origins of both folds, and, finally, we will present a model for the formation of the whole elongated domal system.

6.1. Extensional Detachments and N-S Trending Folds

[25] In the elongated domes of the Sierra de los Filabres and Sierra Nevada, anticlinal axes trending N-S to NNE-SSW are roughly perpendicular to the average direction of extension of the detachments (both the Mecina and the Filabres detachments). These folds are particularly well developed in the western Sierra Nevada, where the highest topographic elevations occur (Figure 9). Moreover, taking into account their westerly position in the Nevado-Filabride outcrop with respect to the sense of movement of the hanging wall along the detachments (roughly WSW), these longitudinal folds (in

the sense of *Janecke et al.* [1998]) could be interpreted as a rolling-hinge anticline [see *Axen and Bartley* [1997]. Other observations also support this interpretation, namely, (1) the folds affect the detachments and are confined to the lower plate rocks of the two extensional systems (i.e., the Nevado-Filabride units in western Sierra Nevada; Figures 1 and 2); (2) their interlimb angle decreases and their fold amplitude increases westward, in agreement with the fold geometry observed in other field examples and predicted in rolling-hinge models [e.g., *Manning and Bartley*, 1994; *Wdowinski and Axen*, 1992; *Axen et al.*, 1995; *Dinter*, 1998]; and (3) cooling to near-surface temperatures becomes progressively younger in footwall rocks toward the west; it occurred during the middle Serravallian in eastern Sierra de los Filabres (12 ± 1 Ma) and was completed by the early Tortonian in western Sierra Nevada (9–8 Ma) [*Johnson*, 1997; *Johnson et al.*, 1997]. Younging in cooling ages in the direction of slip is consistent with the progressive tectonic denudation of footwall rocks and rolling-hinge folding below crustal-scale extensional detachments [e.g., *Foster et al.*, 1993; *John and Foster*, 1993; *John and Howard*, 1995; *Howard and Foster*, 1996].

[26] The trend of some of these longitudinal folds (NNE-SSW), nevertheless, is not strictly perpendicular to the direction of extension (WSW-ENE) deduced from striations, grooves, and other slickenlines in fault surfaces and shear bands (Figures 2 and 5), although they are subparallel to the footwall cutoff lines of the detachment surfaces (Figure 8a). The obliquity (≈70°–80°) between the footwall cutoff lines and the direction of extension indicates that the extensional detachments are oblique with a left-handed strike-slip component of displacement. This observation supports our case in naming the folds with respect to their cutoff lines, regardless of their angular relationships with the direction of extension. In this case, longitudinal folds designate folds approximately parallel to footwall cutoff lines.

[27] There are two end-member kinematic models to explain rolling-hinge footwall uplift in response to extension: (1) subvertical simple shear, as might result from local Airy isostatic compensation [*Axen and Wernicke*, 1991; *Axen et al.*, 1995], or (2) elastically controlled deformation (by flexural failure), where the footwall is treated as a viscous plate [*Buck*, 1988, 1993; *Weissel and Karner*, 1989; *Block and Royden*, 1990; *King and Ellis*, 1990; *Lavier et al.*, 1999]. The two mechanisms predict a different deformation history and structures, although there is a general consensus that they need not be mutually exclusive [*Manning and Bartley*, 1994; *Axen and Bartley*, 1997]. In our case, several observations favor the simple shear model: (1) the near-vertical dip of the axial plane of the rolling-hinge anticline in western Sierra Nevada (Figure 7); (2) the presence of small-scale folds, with both SE and NW vergence, trending subparallel to this anticline [*Galindo-Zaldívar*, 1993]; and (3) the occurrence of pervasive, postmylonitic subvertical joints in the proximity of this fold. The absence of structures denoting the occurrence of layer-parallel slip and the lack of a conjugate set of faults (both west down and east down faults) would be, in addition, more indicative of unroofing via subvertical simple shear rather than via elastic processes [*Selverstone et al.*, 1995, Figure 1].

[28] On the other hand, there are abundant high-angle, west dipping (i.e., synthetic) normal faults that produced a net extension parallel to the regional foliation (e ≈ 0.25; Figure 10). These structures most likely result from the combination of isostatically induced stresses in the hinge zone with far-field extensional stresses driven by the movement of the detachments. This combination would cause net horizontal extension in the footwall, which can produce synthetic faulting accompanying subvertical shear structures [*Manning and Bartley*, 1994; *Axen et al.*, 1995]. However, for this combination of local and far-field stresses, *Manning and Bartley* [1994] showed that synthetic faulting must be small compared with subvertical structures, younger faults would be steep, their cutoff angles with the regional footwall foliation should be small (approximately <20°–30°) and, once the footwall surpasses the rolling hinge, foliation would dip subhorizontally or toward the detachment (i.e., westerly). Many of these predictions fail in our case, because the faults dip moderately toward the west (≈40°) and have relatively high cutoff angles (≈45°). The gentle eastward dip of the foliation (≈15°) on the eastern side of these faults (i.e., once they have passed through the rolling hinge; Figure 10) suggests that apart from a deviation of isostatically driven simple shear from the vertical as a result of interaction with far-field extensional stresses, other processes were also taking place in the region. We interpret one of these processes as being represented by new detachments, which backcut the footwall (i.e., toward the east), generate rollover folds, and accentuate the dip of the eastern fold limb of the rolling-hinge anticline, diminishing its interlimb angle.

[29] The calculated prolongation to depth of one of these faults (Figure 10), using several length-balancing methods to determine fault shapes in-depth (in particular the *Suppe* [1983] method or the inclined, synthetic shear-constant heave method of *Jackson and Galloway* [1984]), suggests they must flatten out at 13–15 km. The determined fault shape is consistent with the depth-distribution of recent earthquake hypocenters in the westernmost Sierra Nevada area (from *Serrano et al.* [1996] and *Morales et al.* [1997]) and with the brittle-ductile transition deduced from a strength profile calculated using local heat flow data taken from *Fernàndez et al.* [1998]. Seismicity, strength estimates, and surface structural data clearly indicate that the Mecina and Filabres detachment systems are currently inactive and that a new, active extensional detachment deforms a previous rolling hinge structure (Figure 10). This interpretation is in disagreement with previous suggestions by other authors, who postulate that the Mecina detachment continues deepening further to the west, is still active, and determines present-day upper crustal seismicity [e.g., *Galindo-Zaldívar et al.*, 1997, 1999].

[30] If we assume that the subvertical simple shear model could essentially explain this rolling-hinge structure, the original dip of the detachment systems can be reconstructed. This value can first be estimated using the interlimb angle (Θ = 68°; see Figure A3) of the domal antiform shown in Figure 7. Using the geometrical relationships presented in Appendix A, the initial dip of the detachment is ≈32° (i.e., 90–Θ). We can also improve the precision of this estimate by using the footwall cutoff angles of the detachment systems. The footwall cutoff angles observed in the central Sierra de los Filabres are 15°–18°, which is the average regional dip (toward the east) of the foliation in that region. In the western Sierra Nevada, footwall mylonitic rocks and the Mecina and Filabres extensional systems themselves dip ∼27°–30° west on average. The latter angles represent the maximum original dip of both detachments, as they are at the top of the limb that has not yet passed the rolling hinge anticline. The difference between these values (27°–30°) and the cutoff angles measured in the eastern sector of the section (15°–18°) can be interpreted as (1) an original feature of the detachment

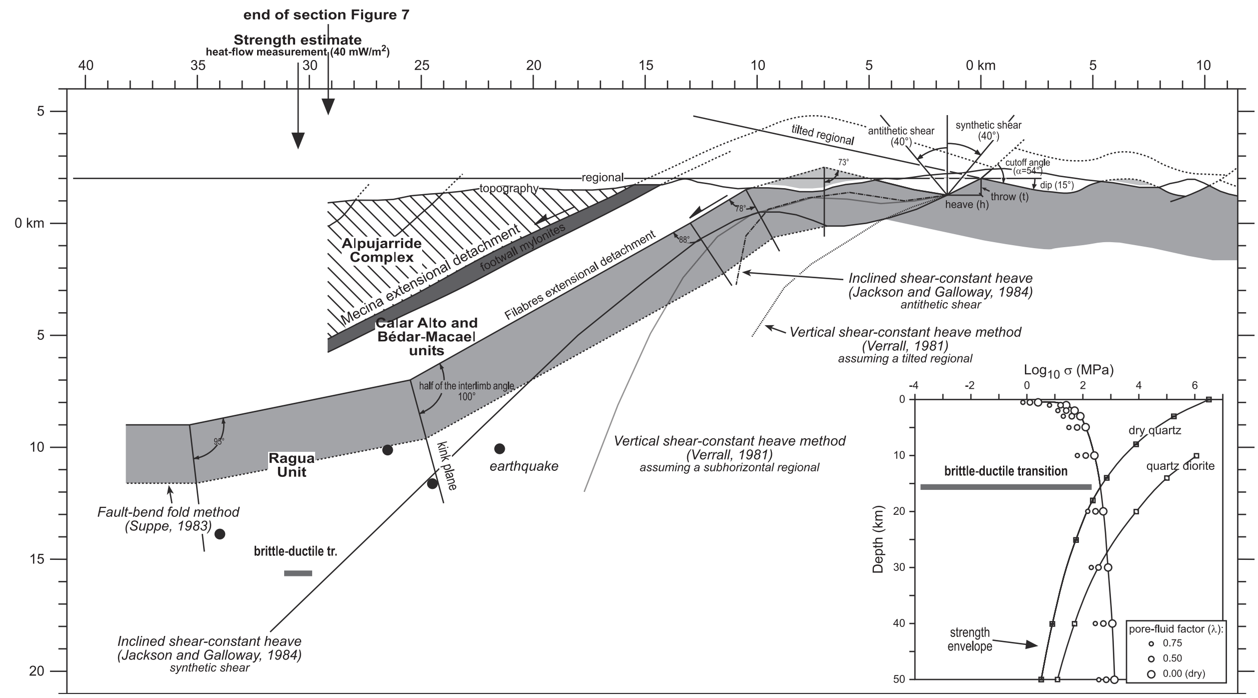

Figure 10. Prolongation to depth of the normal fault located on the western slope of the Picón de Jeres (Figures 2 and 6) using the following length-balancing methods: the fault bend method [*Suppe*, 1983]; the inclined shear, constant-heave method, using either a synthetic or antithetic shear of 40° [*Jackson and Galloway*, 1984; *White et al.*, 1986; *Dula*, 1991]; and the vertical shear, constant-heave method [*Verrall*, 1981; *Gibbs*, 1983]. The strength envelope is calculated for local heat flow data (40 mW/m^2) in western Sierra Nevada [*Fernàndez et al.*, 1998], following the method described by *Ranalli* [1987], assuming normal faulting, and using the creep parameters of *Lynch and Morgan* [1987], for the upper (dry quartz) and lower (quartz-diorite) crust.

systems consisting of an imbricated listric fan, comprising progressively younger and steeper faults away from the initial fault breakaway or, alternatively, (2) an indication of the maximum change in the footwall surfaces as they passed trough the rolling hinge. In the latter case, bending at the rolling-hinge anticline was certainly <12°, in agreement with the small amount of bending (<5°–10°) estimated in other low-angle normal faults [*Axen et al.*, 1995; *Axen and Bartley*, 1997]. The initial dips of the detachment systems were, in summary, probably <27°–30°. We suggest that the Mecina and Filabres detachments presently flatten above 13–15 km depth, which corresponds to the depth where a new and active detachment seems to root. This depth would also correspond to the maximum depth of the lower hinge of the ramp (rolling-hinge syncline). Using the horizontal extension estimated above (109–116 km, see Appendix A) and the suggested initial dip of the detachment faults, we deduce an average downdip displacement of about ∼122–134 km. Such a high amount of extension, common to other low-angle normal faults [e.g., *Wernicke*, 1992], is possible for faults initially dipping <20° [*Forsyth*, 1992] (Figure 7).

[31] The total extension (109–116 km) produced by the two detachment systems was accommodated by upward doming in the upper crust, with lateral and vertical flow of all the Nevado-Filabride section initially situated below 10 km. Any rolling-hinge model requires an intracrustal level of compensation to explain crustal flow and a final subhorizontal Moho geometry in regions under differential values of extension [*Block and Royden*, 1990; *Melosh*, 1990; *Wdowinski and Axen*, 1992; *Wernicke*, 1992]. The presence of a subhorizontal Moho under the core complex [e.g., *Banda et al.*, 1993], the absence of any geological or geophysical evidence to suggest the participation of magmatic flow from the mantle of the right age and amount under these elongated domal structures [e.g., *Torne et al.*, 2000], together with the observation of a subhorizontal intracrustal discontinuity in deep seismic profiling [*García-Dueñas et al.*, 1994; *Martínez-Martínez et al.*, 1997a], have been used by *Martínez-Martínez et al.* [1997b] to suggest that these domes are compensated in depth by the lateral and vertical influx of buoyant midcrustal material, fluid in an asthenospheric sense [*Wernicke*, 1990, 1992]. The compensation depth would most likely have occurred above a prominent midcrustal decoupling level that is presently at 16.5–21 km (Figure 11).

[32] Another intriguing aspect is the elevation achieved by the anticline culmination in the western Sierra Nevada (>3 km high), since the different mechanical models developed to explain the evolution of topography, footwall and detachment geometries during tectonic denudation predict that footwall rocks should reach maximum average elevations in the range of 1–1.7 km with a gentle topography [*Sonder et al.*, 1987; *Block and Royden*, 1990; *Kruse et al.*, 1991; *Wdowinski and Axen*, 1992; *Stüwe and Barr*, 2000]. The age and the westerly younging direction of the fission track cooling ages [*Johnson*, 1997; *Johnson et al.*, 1997] indicate a short tectonic unroofing of the Nevado-Filabride units, progressing toward the west, from the middle Serravallian (12 ± 1 Ma) to early Tortonian (9–8 Ma). A comparable short-lived or ‘‘catastrophic’’ (in <5 Ma) denudation has recently been found in other extensional

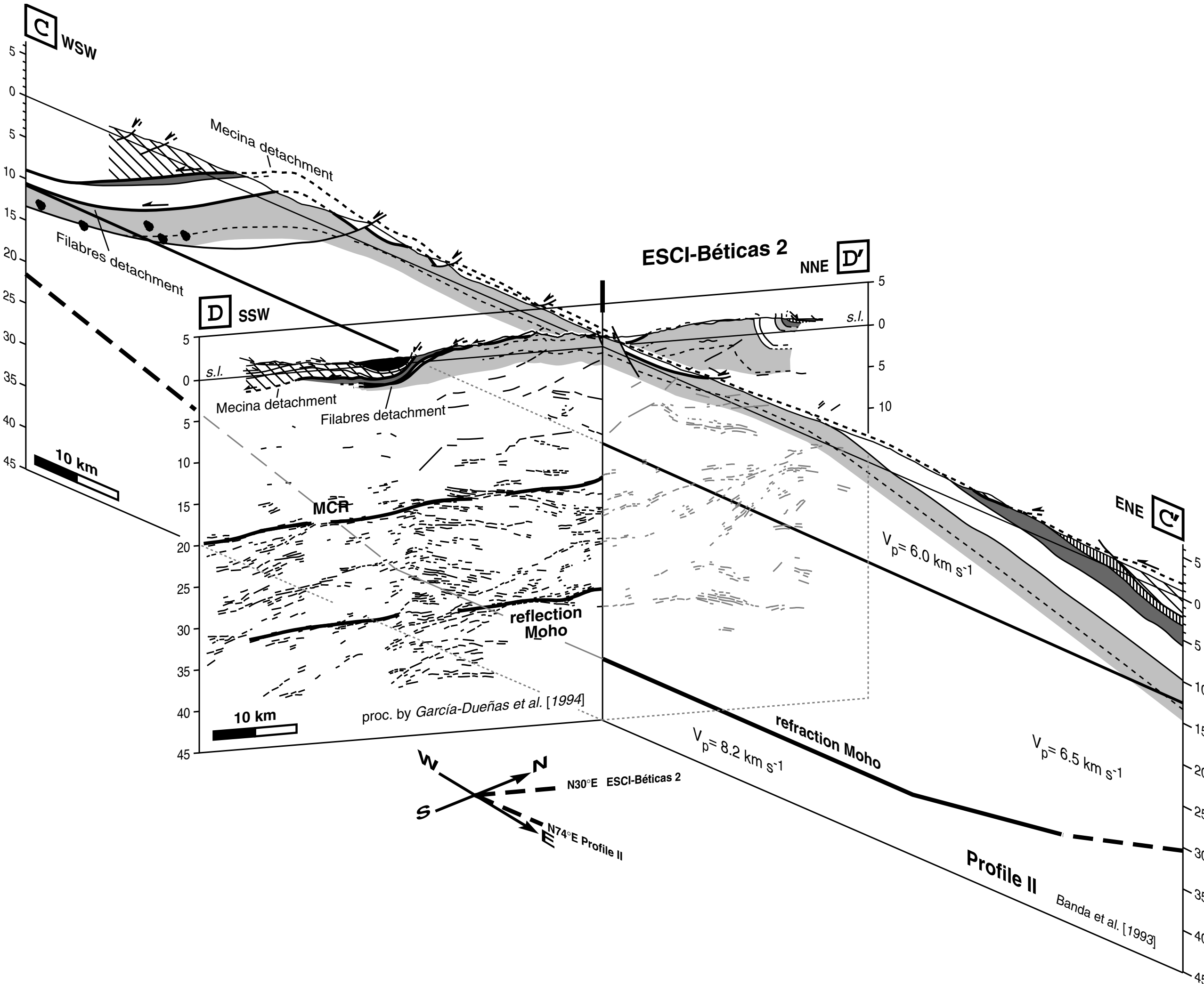

Figure 11. Three-dimensional diagram showing the upper and deep crustal structure of the Sierra Nevada elongated dome, from surface geology and deep-seismic reflection and refraction profiling. Locations of upper crustal cross sections (C-C′ and D-D′) are in Figure 1. Refraction profile (Profile II), trending subparallel to the direction of extension, is taken from *Banda et al.* [1993]. A simplified line drawing of the deep-seismic reflection profile, ESCI-Béticas 2, is shown with a tentative depth-conversion from *García-Dueñas et al.* [1994]. In the lower upper crust there is a marked subhorizontal discontinuity (for example the MCR reflector), which has been interpreted as a midcrustal decoupling level [*Martínez-Martínez et al.*, 1997b]. Above this level, lateral and vertical flow of a buoyant crust occurred during the formation of the elongated dome.

detachment systems [e.g., *Foster et al.*, 1993; *John and Howard*, 1995; *Beutner and Craven*, 1996; *Craddock et al.*, 2000].

6.2. E-W Trending Folds

[33] In contrast to the localized westerly location of the N-S, longitudinal folds, E-W trending, large-scale, open folds have been recognized and described throughout the region. Although these folds have been interpreted as lateral folds formed by the collapse of culmination structures over west directed thrusts [*Frizon de Lamotte et al.*, 1989, 1995] or even as real isostatic structures due to tectonic unroofing below detachment faults [*Galindo-Zaldívar et al.*, 1989; *Galindo-Zaldívar*, 1993], other authors interpret them as folds produced in a N-S contractional event [e.g., *Platt et al.*, 1983; *Weijermars et al.*, 1985; *Crespo-Blanc et al.*, 1994; *Martínez-Martínez et al.*, 1997a]. The first two interpretations can be discarded since no related fold-parallel, west directed thrusting structures are observed in the region, nor is the current elevation (>2 km) and nature (deposited under shallow-marine conditions) of the Serravallian synrift, marine sediments [*Martínez-Martínez and Azañón*, 1997] consistent with a single isostatic origin for the folds.

[34] There are different arguments to support the contractional origin of the E-W folds and their timing: (1) These folds are subparallel to the direction of extension of the two detachment systems; (2) E-W folds have generally north facing asymmetric shapes and affect the sediments and both the lower and upper detachment plates; (3) north vergent reverse faults associated with these folds, as is common on the northern slopes of the Sierra de los

Filabres, where, in addition, large-scale, down-slope gravitational gliding and related structures have been reported [*Voet*, 1964; *Leine*, 1966; *Langenberg*, 1973; *Orozco et al.*, 1999]; (4) paleostress estimates suggest approximate NNW-SSE, constant contraction since the Tortonian in nearby areas [*Estévez and Sanz de Galdeano*, 1983; *Galindo-Zaldívar et al.*, 1993, 1999; *Stapel et al.*, 1996; *Herraiz et al.*, 2000]; and (5) upper Miocene (upper Tortonian to Messinian) to lower Pliocene sediments were deposited in the surrounding Neogene basins (e.g., the Tabernas, Sorbas, and Almanzora basins) under shallow-marine to continental conditions, indicating simultaneous uplift and folding of the surrounding mountain ranges [e.g., *Kleverlaan*, 1989; *Ott D'Estevou and Montenat*, 1990; *Fernández and Guerra-Merchán*, 1996; *Martín and Braga*, 1996; *Pascual*, 1997; *García-García et al.*, 1999]. The subsidence history reconstructed in some of these basins reveals an abrupt change in the shallow-marine sedimentation during the upper Tortonian, which became continental, with an estimated uplift rate of 0.1 – 0.3 mm/yr [*Soria et al.*, 1998; *Rodríguez-Fernández et al.*, 1999].

[35] A fold profile of the two major antiforms in the region (coinciding with the Sierra Nevada and the Sierra de los Filabres topographic culminations) (D-D′ in Figure 11) shows a deduced total N-S shortening of 8 km. Structural data, constrained by deep-seismic reflection profiling along this section, were used by *Martínez-Martínez et al.* [1997a] to suggest a fault bend fold and fault propagation fold structure. The two aforementioned antiforms therefore correspond to hanging wall anticlines related to footwall ramps.

[36] The contractional origin of the E-W trending folds could explain some of the open questions in the previous section regarding the origin of N-S trending folds. A late uplift stage during this N-S contractional episode would explain the following key observations: (1) the current elevation of the rolling hinge anticline in western Sierra Nevada (fold hinge of the Filabres detachment at ≈3 – 3.5 km high, Figure 10); (2) the final geometry of the two detachment systems with two major open and north facing folds; together with (3) the final elevation above sea level (on average ≈1 – 1.5 km high) of the Serravallian-Tortonian coarse conglomerates deposited above the detachment systems, once they were isostatically readjusted. Moreover, the contribution to the topography of this folding event would explain how regions with maximum unroofing (e.g., the highly extended central domains; see striped band in Figure 8b) have both maximum and minimum elevations and why in parts of these areas, E-W synclines were nucleated, yielding a relative maximum sinking (e.g., Fiñana syncline). The 1 – 1.5 km high, final elevation of the sediments deposited over the detachment faults cannot be used to directly estimate the uplift related to the E-W folding event. Until the contribution of a likely isostatic component to the recent tectonics of the region can be quantified, the contribution to the surface uplift of the E-W folding will remain incompletely understood.

6.3. Model for the Origin of the Elongated Domal Structure

[37] The final geometry of these domes is characterized by two main observations: (1) the doubly plunging geometry of both the N-S and E-W trending folds and (2) the extension-parallel (E-W) elongated geometry of the folds, which is particularly well depicted in domal culminations, formed by the interference between two antiforms, as for example in the western Sierra Nevada between the rolling hinge and the E-W anticlines.

[38] Several implications can be deduced for the timing of the two folding events on the basis of a review of the fission track ages from the region (published by *Johnson et al.* [1997] and *Johnson* [1997]) and taking into account the new kinematic and structural data provided here: (1) Near-surface cooling ages from the N-S trending rolling-hinge anticline in western Sierra Nevada occurred during the uppermost Tortonian and Messinian (average ages are 9.4 ± 0.9 Ma for zircon and 5.2 ± 2.3 Ma for apatite); (2) along the major, E-W, antiformal axial traces of Sierra Nevada and Sierra de los Filabres, fission track ages tend to be younger toward the west and contemporaneous with the middle Miocene (Serravallian; 13 – 10.5 Ma) extensional episode, (3) whereas in N-S traverses across E-W anticlines, fold cores were systematically exhumed before their adjacent limbs, which are progressively younger to the west, from middle Serravallian in eastern Sierra de los Filabres to Messinian in eastern Sierra Nevada (average apatite ages in E-W fold limbs are 9.1 ± 2.6 Ma and 5.7 ± 1.3 Ma, respectively); and (4) finally, extension is still active in western Sierra Nevada, where a west directed listric detachment, postdating the Filabres and Mecina extensional systems, seems to control the shallow crustal seismicity in the eastern Granada basin (Figure 10).

[39] These observations certainly indicate that the age of E-W folding becomes progressively younger toward the west, from middle Serravallian to middle Tortonian (≈9Ma) in the eastern Sierra de los Filabres, to uppermost Tortonian and Messinian (and even lower Pliocene) (≈6Ma) in its western sector and in the eastern Sierra Nevada. This interpretation is also consistent with the distribution and age of sediments in the region, where the first occurrence of Nevado-Filabride detritus are marine middle Serravallian sediments in the north of the eastern Sierra de los Filabres [*Lonergan and Mange-Rajetzky*, 1994], shallow-marine to continental, lower Tortonian sediments in the Tabernas basin [e.g., *Pascual*, 1997], and shallow-marine to continental, uppermost Tortonian to lower Pliocene in the western Sierra Nevada and in Granada basin (Figure 1) [*Rodríguez-Fernández and Sanz de Galdeano*, 1992; *García-García et al.*, 1999].

[40] E-W folding progressed therefore in a similar fashion to the extensional unroofing, i.e., toward the west. We suggest that E-W folding started to take place in areas behind the extensional unroofing, coexisting, from the middle Serravallian to the uppermost Tortonian and Pliocene, with tectonic denudation (related to the low-angle extensional detachments and the rolling-hinge antiform in a westerly position). Perpendicular contraction also occurred at the same time behind the extensional front, both progressing toward the west. This system would have produced progressive superposition and migration toward the west of contractional structures in previously extended domains, uplifting the inactive and isostatically readjusted portions of the low-angle detachment systems and their relative lower plate rocks.

[41] The inferred compression perpendicular to the direction of extension requires the consideration of three-dimensional models to explain the formation of this dome-and-basin geometry [e.g., *Axen et al.*, 1998]. Taking into account the model presented by *Yin* [1991], the geometry and dominant wavelength (55 – 70 km and 20 – 25 km, measured parallel and perpendicular to the direction of extension, respectively) of these elongated domes (Figure 8b) could have formed with a thin effective elastic crust,

probably <10 km, a relatively high ratio between deviatoric extension-parallel and perpendicular stresses, and a laterally changing vertical load. Lateral variations in the vertical force could be due to the existence of an uncompensated and nonuniform crustal root during extension [*Yin*, 1991]. Present-day crustal thickness under the Sierra Nevada and Sierra de los Filabres region [*Torne et al.*, 2000], moreover, demonstrates that these domes are built over a crust that distinctly thins toward both the east and south. If some of these crustal thickness variations occurred during the middle Miocene, a complex distribution of laterally changing vertical forces would have accompanied the extension, enhancing domal-forming processes. On the other hand, lateral variations in the vertical forces could also be produced by the NNW-SSE plate convergence boundary conditions during the west directed asymmetric extension, still active after the footwall was significantly unloaded. The middle-Miocene to Pliocene formation of the Sierra Nevada elongated dome at the core of the Betic hinterland therefore constitutes another example of the coexistence of extension and contraction during continued overall convergence and mountain building.

7. Conclusions

[42] The following points summarize our conclusions.

1. Miocene extension and consequent exhumation of the lower metamorphic complexes in the hinterland of the Betics was accommodated by two sequentially developed WSW directed extensional detachments associated with low-angle normal faults. Both detachments have an overall low-angle ramp geometry cutting their respective footwalls downsection toward the west. They were initially shallowly dipping faults, initial dip probably <27°–30°, being active during a short period of time (from 12 to 8 Ma), as indicated by fission track data.

2. The total amount of extension across the core complex is ~109–116 km ($\beta \approx 3.5$–3.9), according to the distance between the axial surfaces of faulting-related folds in the lower plate (distal antiform and proximal synform hinges) and using a geometrical model for subvertical simple shear deformation during footwall denudation.

3. Extensional detachments, together with their respective footwall reference surfaces, are similarly folded, showing an E-W elongated dome-and-basin noncylindrical geometry (doubly plunging upright or box-shaped open en echelon folds with amplitude of ≈6 km and half wavelength of ≈30 km, and longitudinal to transverse wavelength ratio of 1.5–3). Antiformal axial surface traces run subparallel or coincide with the main topographic culminations of the region, where the maximum elevations of the Iberian Peninsula are found (e.g., the Mulhacén and Veleta peaks, at 3482 and 3398 m, respectively). This suggests a close link between the structural relief of these domes and the topography. Elongated domes are interpreted as being formed by interference between two suborthogonal fold sets, trending subperpendicular and subparallel to the direction of extension (WSW-ENE).

4. The longitudinal folds are interpreted as forming part of a rolling-hinge anticline taking into account the westerly position and abundance of the longitudinal (N-S) folds in the Sierra Nevada elongated dome, their angular relationships to the direction of extension (subparallel to footwall cutoff lines), their confinement to the detachments and their respective lower plates, and the decrease in the interlimb angle and increase in the fold amplitude, both westward. Other structural observations suggest a subvertical simple shear mechanism (interacting with far-field stresses) to form this rolling-hinge anticline, with a relatively small degree of bending (<5°–10°) as footwall rocks passed through it. The age of this longitudinal fold set is still not well constrained, although available fission track cooling ages [*Johnson*, 1997; *Johnson et al.*, 1997] indicate simultaneous longitudinal folding as the extensional unroofing took place (i.e., mid-Serravallian to late Tortonian). Several lines of evidence suggest a contractional origin for the E-W folds, namely, (1) they are north facing asymmetric folds; (2) they affect the overlying sediments and both lower and upper detachment plates; and (3) they control the present-day topography, determining an overall surface uplift once the extensional detachments unroofed footwall rocks to near sea level.

5. We conclude that orthogonal folding of detachment faults and their respective footwalls is produced by the interference between a westerly moving rolling-hinge anticline and E-W folding behind the extensional front, progressively affecting to the west the isostatically readjusted segments of the detachments once they are inactive. This system was active from the Serravallian to the lower Pliocene, and extension is still active from the rolling-hinge anticline in Sierra Nevada to the west. The mid-Miocene to Pliocene formation of the Sierra Nevada elongated dome at the core of the Betic hinterland therefore constitutes another example of the coexistence of extension and contraction during continued overall convergence and mountain building.

Appendix A: Extension Calculation Using Rolling-Hinge Geometries

[43] Assuming a distributed subvertical simple shear mechanism to form rolling-hinge structures, *Axen and Wernicke* [1991] first analyzed the geometry of footwall uplift resulting from tectonic denudation along low-angle normal faults. Footwall uplift in this model results in local isostatic compensation (or pure Airy), as contrasted with plate-bending behavior in the elastic-plastic flexural-failure model [e.g., *Block and Royden*, 1990; *Manning and Bartley*, 1994]. In simple staircase normal fault geometry, and assuming that the hanging wall block is rigid, they showed how four axial surfaces form upon the onset of faulting and how finite strain in footwall rocks is directly related to fault dip, determining layer-parallel thinning (and antithetic reverse shearing) followed by thickening (and synthetic normal shearing) as footwall denudation progresses, passing through the rolling-hinge anticline. We have expanded the model presented by *Axen and Wernicke* [1991] in order to evaluate horizontal extension using the final geometry of the rolling-hinge structure.

[44] Figure A1 shows the evolution of a rolling-hinge structure with progressive extension along a hypothetical low-angle normal fault (α, fault dip). For the sake of simplification we assume that this fault has a simple staircase geometry, with a gently dipping ramp ($\alpha = 30°$ toward the left) and flattens out at depth, *z*. In the reconstruction in Figure A1, this depth is shown at 15 km, coinciding with the brittle-ductile transition calculated in the area (see Figure 10). Since the start of faulting, four axial surfaces have formed, linked to the top and bottom of the ramp in the footwall (axial surfaces A and B) or in the hanging wall (C and D). As pointed out by *Axen and Wernicke* [1991], the two axial surfaces

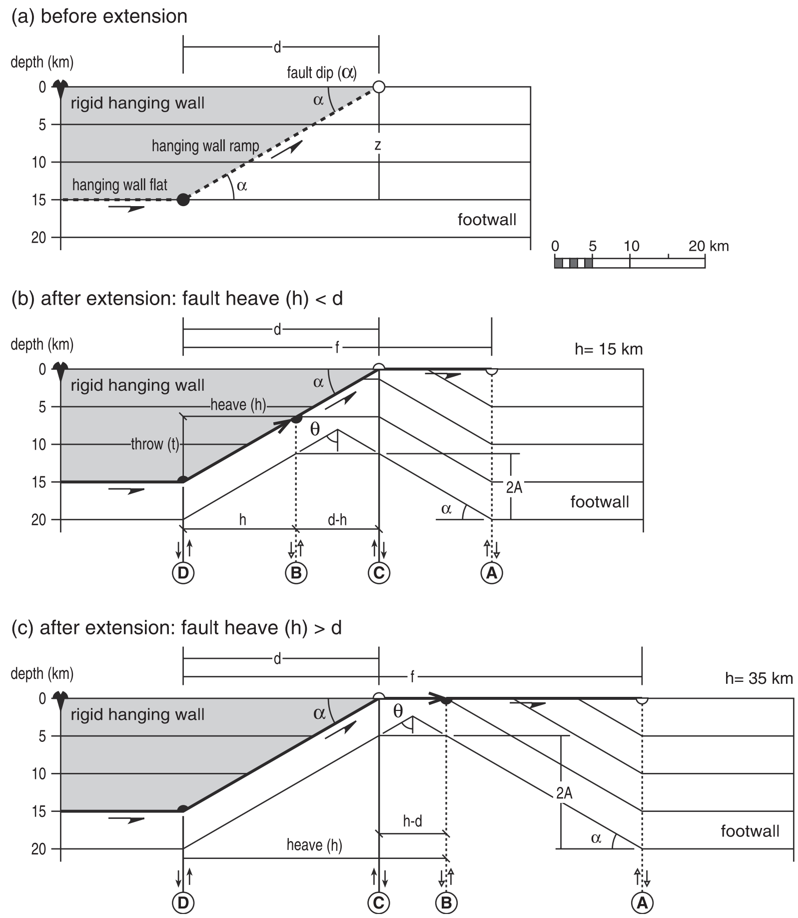

Figure A1. Evolution of a rolling-hinge structure in the footwall of an extensional detachment, initially dipping 30° and flattening out in the brittle-ductile transition at 15 km depth. Axial surfaces are marked with circled capital letters. Model of footwall deformation is vertical simple shear.

tied to the footwall were only active at the onset of faulting, affected only surrounding footwall rocks, and subsequently lay passively in the footwall. Axial surface C, at the top of the hanging wall ramp, corresponds to the rolling-hinge structure as all the footwall rocks pass through it as they are unroofed.

[45] The amount of horizontal extension can be estimated with respect to the horizontal projection of the fault ramp, prior to faulting (d) or after faulting (f). The distance, f, corresponds to the horizontal distance between the bottom ramp of the hanging wall (solid half-circle) and the exhumed, upper ramp in the footwall (open half-circle). The amount of horizontal extension (e) or the stretching factor (β) could therefore be related to the dip-slip component of the fault, given by the vertical component (or fault throw, t) and to the horizontal component of dip slip (or fault heave, h) by

$$e = \frac{f - d}{d} = \frac{h}{d} \tag{1}$$

$$\beta = \frac{f}{d} = 1 + \frac{h}{d}. \tag{2}$$

These parameters can also be expressed as a function of the fault dip (α), considering the depth at which the fault flattens out (z), by the following expressions:

$$e = \frac{h \tan \alpha}{z} \tag{3}$$

$$\beta = 1 + \frac{h \tan \alpha}{z}. \tag{4}$$

As shown in Figure A1, the fault heave (h) coincides with the horizontal distance between the upper footwall and hanging wall ramps (distance AC; open half-dots), or the relative lower ramps (distance BD; solid half-dots). The first of these distances can be simply estimated in extension-parallel cross sections, because it corresponds to the distance between the rolling anticline and the passive synform linked to the footwall at the initial fault breakaway.

[46] Let us first calculate the width of the dome culmination (w), which always turns out to be the distance between the lower footwall and the upper hanging wall fault ramps (B and C, respectively). When the fault heave is lower than d (Figure A1b), this width is

$$w = d - h, \tag{5}$$

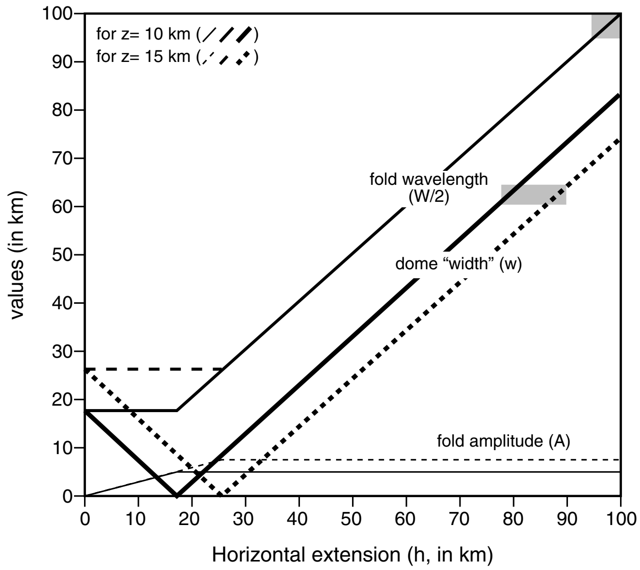

Figure A2. Evolution of the fold amplitude (A), half of the fold wavelength ($W/2$), and dome "width" (w) parameters as a function of horizontal extension (fault heave, h), for faults with constant dip of 30° and flattening out at two different depths of brittle-ductile transition (10 and 15 km). Shaded boxes show the fold values measured in the section of Figure 7 (see also Figure A3).

whereas when it is larger than d (Figure A1c), it is

$$w = h - d. \tag{6}$$

These two equations can also be given as a function of the fault dip by the following relative expressions:

$$w = \frac{z}{\tan \alpha} - h \tag{7}$$

and

$$w = h - \frac{z}{\tan \alpha}. \tag{8}$$

The shape of the resulting dome, comprised of the four axial surfaces, can be defined by the fold amplitude (A) and half of the fold wavelength ($W/2$). These geometrical parameters can be deduced by using the trigonometric relationships depicted in Figure A1 and expressions (5) to (8). For low amounts of extension ($h < d$), these fold parameters are

$$\frac{W}{2} = 2\frac{h}{2} + w = d = \frac{z}{\tan \alpha} \tag{9}$$

and

$$A = \frac{h \tan \alpha}{2} = \frac{hz}{2d} = \frac{t}{2}, \tag{10}$$

whereas for higher amounts of extension ($h > d$), they are given by

$$\frac{W}{2} = 2\frac{d}{2} + w = h = \frac{z}{\tan \alpha} + w \tag{11}$$

and

$$A = \frac{d \tan \alpha}{2} = \frac{z}{2}. \tag{12}$$

It should be noted that in this model the interlimb angle (half of the interlimb angle equals Θ) of the domal antiform remains constant, regardless of the amount of extension or of the reference surface taken in the footwall, at it is exclusively a function of the fault dip ($\Theta = 90 - \alpha$).

[47] To illustrate the variations in these relationships with the amount of horizontal extension, we have represented in Figure A2

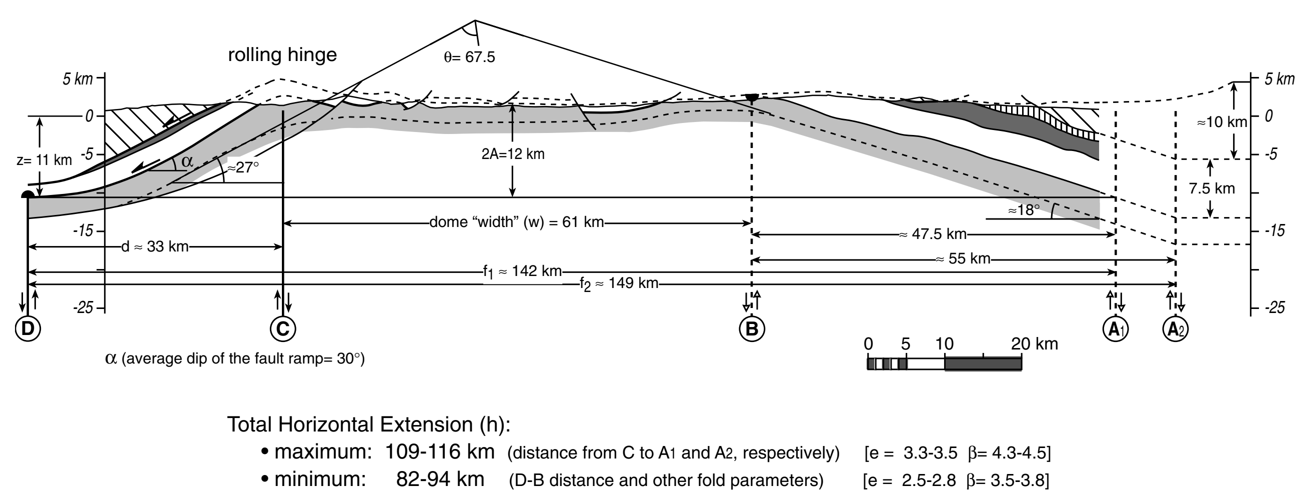

Figure A3. Extension-parallel cross section (simplified from Figure 7) showing the different fold parameters used to estimate the total horizontal extension, applying the equations of Appendix A.

the geometry of a domal structure in the footwall of a low-angle normal fault, dipping 30°, and flattening out at two different brittle-ductile transition depths (placed at reasonable depths of 15 km and 10 km). It can be seen that the domes resulting from this rolling-hinge model are upright and with a box-fold shape, tending to have a narrower (w decreases and $W/2$ remains constant) and more pointed culmination (A increases; $A \leq z/2$), that it is producing a more chevron-like fold, as extension comes closer to the critical value d. In contrast, for higher amounts of extension, domes become progressively broader (w and $W/2$ increase), with a constant fold amplitude ($A = z/2$). The critical extension value ($d = h$), where domes become chevron-like folds, with a maximum amplitude and a minimum fold wavelength, is a function of the depth, z ($h = z/\tan \alpha$), at which the fault flattens out.

[48] In summary, the shape of the dome formed by the rolling-hinge subvertical simple shear mechanism, observed in an extension-parallel cross section, can be used to estimate the amount of horizontal extension, once the location of the four axial surfaces and the fault geometry are adequately constrained. The principal observations used to estimate the amount of horizontal extension in our case are summarized in Figure A3, a simplification of the cross section shown in Figure 7. Using the geometrical relationships described previously in Appendix A, and assuming that this rolling-hinge mechanism is governing dome genesis (see section 5), we estimate a horizontal extension ranging from ~82–94 km to 109–116 km (β = 3.5–3.8 to 4.3–4.5, respectively). The higher estimate comes from introducing the distance between the axial surfaces C (the rolling-hinge anticline) and A (the passive-hinge syncline) (f = 142–149 km; d = 33 km), and the fold wavelength ($W/2$ = 102 km) in equation (11). If, in the same expression, we use the dome "width" (w = 61 km) and the fault dip (α = 30°) values, we obtain a smaller estimate of horizontal extension. Measured fold amplitude ($2A$ = 12 km) corresponds to the depth at which the detachment fault flattens out (equation (12)), in close agreement with our geometrical reconstruction of this depth (z = 11 km) shown in Figure A3.

[49] **Acknowledgments.** Financial support for this work was provided by projects MAR98-0981 and BTE2000-0581 (CICYT). We thank Craig Jones, Neil Mancktelow, Jon Spencer, and the editor, Brian Wernicke, for their constructive reviews and advice on improving the manuscript.

References

Amato, J. M., J. E. Wright, P. B. Gans, and E. L. Miller, Magmatically induced metamorphism and deformation in the Kigluaik gneiss dome, Seward Peninsula, Alaska, *Tectonics*, *13*, 515–527, 1994.

Anderson, R. E., T. P. Barnhard, and L. W. Snee, Roles of plutonism, midcrustal flow, tectonic rafting, and horizontal collapse in shaping the Miocene strain field of the Lake Mead area, Nevada and Arizona, *Tectonics*, *13*, 1381–1410, 1994.

Axen, G. J., and J. M. Bartley, Field tests of rolling hinges: Existence, mechanical types, and implications for extensional tectonics, *J. Geophys. Res.*, *102*, 20,515–20,537, 1997.

Axen, G. J., and B. P. Wernicke, Comment on "Tertiary extension and contraction of lower-plate rocks in the Central Mojave metamorphic core complex, Southern California" by John M. Bartley, John M. Fletcher, and Allen F. Glazner, *Tectonics*, *10*, 1084–1086, 1991.

Axen, G. J., J. M. Bartley, and J. Selverstone, Structural expression of a rolling hinge in the footwall of the Brenner Line normal fault, eastern Alps, *Tectonics*, *14*, 1380–1392, 1995.

Axen, G. J., J. Selverstone, T. Byrne, and J. M. Fletcher, If the strong crust leads, will the weak crust follow?, *GSA Today*, *8*, 1–8, 1998.

Azañón, J. M., and A. Crespo-Blanc, Exhumation during a continental collision inferred from the tectonometamorphic evolution of the Alpujarride Complex in the central Betics (Alborán Domain, SE Spain), *Tectonics*, *19*, 549–565, 2000.

Azañón, J. M., A. Crespo-Blanc, and V. García-Dueñas, Continental collision, crustal thinning and nappe forming during the pre-Miocene evolution of the Alpujarride Complex (Alborán Domain, Betics), *J. Struct. Geol.*, *19*, 1055–1071, 1997.

Bakker, H. E., K. De Jong, H. Helmers, and C. Bierman, The geodynamic evolution of the Internal Zone of the Betic Cordilleras (southeast Spain): A model based on structural analysis and geothermobarometry, *J. Metamorph. Geol.*, *7*, 359–381, 1989.

Balanyá, J. C., V. García-Dueñas, and J. M. Azañón, Alternating contractional and extensional events in the Alpujarride nappes of the Alborán Domain (Betics, Gibraltar Arc), *Tectonics*, *16*, 226–238, 1997.

Banda, E., J. Gallart, V. García-Dueñas, J. J. Dañobeitia, and J. Makris, Lateral variation of the crust in the Iberian peninsula: New evidence from the Betic Cordillera, *Tectonophysics*, *221*, 53–66, 1993.

Bartley, J. M., and B. Wernicke, The Snake Range decollement interpreted as a major extensional shear zone, *Tectonics*, *3*, 521–534, 1984.

Bartley, J. M., J. M. Fletcher, and A. F. Glazner, Tertiary extension and contraction of lower-plate rocks in the Central Mojave metamorphic core complex, southern California, *Tectonics*, *9*, 521–534, 1990.

Beutner, E. C., and A. E. Craven, Volcanic fluidization and the Heart Mountain detachment, WY, *Geology*, *24*, 595–598, 1996.

Biju-Duval, B., J. Dercourt, and X. Le Pichon, From the Tethys ocean to the Mediterranean seas: A plate tectonic model of the evolution of the western alpine system, in *International Symposium on the Structural History of the Mediterranean Basins*, edited by B. Biju-Duval and L. Montadert, pp. 143–164, Technip, Paris, 1977.

Block, L., and L. H. Royden, Core complex geometries and regional scale flow in the lower crust, *Tectonics*, *9*, 557–567, 1990.

Bouchez, J. L., and A. Pêcher, The Himalayan main central thrust pile and its quartz-rich tectonites in central Nepal, *Tectonophysics*, *78*, 23–50, 1981.

Bouillin, J. P., M. Duran-Delga, and P. Olivier, Betic-Rifain and Tyrrhenian Arcs: Distinctive features genesis and development stages, in *The origin of Arcs*, edited by F. C. Wezel, pp. 281–304, Elsevier Sci., New York, 1986.

Brady, R., B. Wernicke, and J. Fryxell, Kinematic evolution of a large-offset normal fault system, South Virgin Mountains, Nevada, *Geol. Soc. Am. Bull.*, *112*, 1375–1397, 2000.

Buck, W. R., Flexural rotation of normal faults, *Tectonics*, *7*, 959–973, 1988.

Buck, W. R., Effect of lithospheric thickness on the formation of high- and low-angle normal faults, *Geology*, *21*, 933–936, 1993.

Buick, I. S., The late Alpine evolution of an extensional shear zone, Naxos, Greece, *J. Geol. Soc. London*, *148*, 93–103, 1991.

Chalouan, A., and A. Michard, The Ghomarides nappes, Rif coastal range, Morocco: A variscan chip in the Alpine belt, *Tectonics*, *9*, 1565–1583, 1990.

Chauvet, A., and M. Séranne, Extension-parallel folding in the Scandinavian Caledonides: Implications for late-orogenic processes, *Tectonophysics*, *238*, 31–54, 1994.

Coleman, D. S., J. M. Bartley, J. D. Walker, D. E. Price, and A. M. Friedich, Extensional faulting, footwall deformation and plutonism in the Mineral Mountains, Southern Sevier Desert, in *Mesozoic to Recent Geology of Utah*, edited by P. K. Link and B. J. Kowallis, *Brigham Young Univ. Geol. Stud.*, *42*(2), 203–233, 1997.

Comas, M. C., V. García-Dueñas, and M. J. Jurado, Neogene tectonic evolution of the Alborán Sea from MSC data, *Geo Mar. Lett.*, *12*, 157–164, 1992.

Comas, M. C., J. P. Platt, J. I. Soto, and A. B. Watts, The origin and tectonic history of the Alborán Basin: Insights from Leg 161 results, *Proc. Ocean Drill. Program. Sci. Results*, *161*, 555–580, 1999.

Craddock, J. P., K. J. Nielson, and D. H. Malone, Calcite twinning strain constraints on the emplacement rate and kinematic pattern of the upper plate of the Heart Mountain Detachment, *J. Struct. Geol.*, *22*, 983–991, 2000.

Crespo-Blanc, A., Interference pattern of extensional fault systems: A case study of the Miocene rifting of the Alborán basement (north of Sierra Nevada, Betic Chain), *J. Struct. Geol.*, *17*, 1559–1569, 1995.

Crespo-Blanc, A., M. Orozco, and V. García-Dueñas, Extension versus compression during the Miocene tectonic evolution of the Betic chain: Late folding of normal fault systems, *Tectonics*, *13*, 78–88, 1994.

Davis, B. K., and R. A. Henderson, Syn-orogenic extensional and contractional deformation related to granite emplacement in the northern Tasman Orogenic Zone, Australia, *Tectonophysics*, *305*, 453–475, 1999.

Davis, G. A., and G. S. Lister, Detachment faulting in continental extension: Perspective from the southwestern U.S. Cordillera, in *Processes in Continental Lithospheric Deformation*, edited by S. P. Clark Jr., B. C. Burchfiel, and J. Suppe, *Geol. Soc. Am. Spec. Pap.*, *218*, 133–159, 1988.

Davis, G. H., and J. J. Hardy, The Eagle Pass detachment, southeastern Arizona: Product of mid-Miocene (?) normal faulting in the southern Basin and Range province, *Geol. Soc. Am. Bull.*, *92*, 749–762, 1981.

Dewey, J. F., M. L. Helman, E. Turco, D. H. W. Hutton, and S. D. Knott, Kinematics of the western Mediterranean, in *Alpine Tectonics*, edited by M. P. Coward, D. Dietrich, and R. G. Park, *Geol. Soc. Spec. Publ.*, *45*, 265 – 283, 1989.

Díaz de Federico, A., M. T. Gómez-Pugnaire, E. Puga, and F. P. Sassi, New problems in the Sierra Nevada Complex (Betic Cordilleras, Spain), *Neues Jahrb. Mineral. Monatsh.*, *10*, 577 – 585, 1979.

Dinter, D. A., Late Cenozoic extension of the Alpine collisional orogen, northeastern Greece: Origin of the north Aegean basin, *Geol. Soc. Am. Bull.*, *110*, 1208 – 1226, 1998.

Docherty, J. I. C., and E. Banda, Evidence fo the eastward migration of the Alborán Sea based on regional subsidence analysis: A case for basin formation by delamination of the subcrustal lithosphere?, *Tectonics*, *14*, 804 – 818, 1995.

Duebendorfer, E. M., and W. D. Sharp, Variation in displacement along strike of the South Virgin-White Hills detachment fault: perspective from the northern White Hills, northwestern Arizona, *Geol. Soc. Am. Bull.*, *110*, 1574 – 1589, 1998.

Dula, W. F. J., Geometric models of listric normal faults and rollover folds, *AAPG. Bull.*, *75*, 1609 – 1625, 1991.

Estévez, A., and C. Sanz de Galdeano, Néotectonique du secteur central des Chaînes Bétiques (Bassins du Guadix-Baza et de Grenade), *Rev. Géogr. Phys. Géol. Dyn.*, *24*, 23 – 34, 1983.

Fernández, J., and A. Guerra-Merchán, A coarsening-upward megasequence generated by a Gilbert-type fan-delta in a tectonically controlled context (upper Miocene, Guadix-Baza Basin, Betic Cordillera, southern Spain), *Sediment. Geol.*, *105*, 191 – 202, 1996.

Fernàndez, M., I. Marzán, A. Correia, and E. Ramalho, Heat flow, heat production, and lithospheric thermal regime in the Iberian Peninsula, *Tectonophysics*, *291*, 29 – 53, 1998.

Forsyth, D. W., Finite extension and low-angle normal faulting, *Geology*, *20*, 27 – 30, 1992.

Foster, D. A., A. J. W. Gleadow, S. J. Reynolds, and P. G. Fitzgerald, Denudation of metamorphic core complexes and the reconstruction of the transition zone, west central Arizona: Constraints from apatite fission track thermochronology, *J. Geophys. Res.*, *98*, 2167 – 2185, 1993.

Frizon de Lamotte, D., J. C. Guézou, and M. A. Albertini, Deformation related to Miocene westward translation in the core of the Betic zone: Implications on the tectonic interpretation of the Betic orogen (Spain), *Geodin. Acta*, *3*, 267 – 281, 1989.

Frizon de Lamotte, D., J. C. Guézou, and O. Averbuch, Distinguishing lateral folds in thrust-systems: Examples from Corbières (SW France) and Betic Cordilleras (SE Spain), *J. Struct. Geol.*, *17*, 233 – 244, 1995.

Galindo-Zaldívar, J., *Geometría de las Deformaciones Neógenas en Sierra Nevada* (*Cordilleras Béticas*), *Monogr. Tierras del Sur*, vol. 8, 249 pp., Univ. de Granada, Granada, Spain, 1993.

Galindo-Zaldívar, J., F. González-Lodeiro, and A. Jabaloy, Progressive extensional shear structures in a detachment contact in the Western Sierra Nevada (Betic Cordilleras, Spain), *Geod. Acta*, *3*, 73 – 85, 1989.

Galindo-Zaldívar, J., F. González-Lodeiro, and A. Jabaloy, Stress and paleostress in the Betic-Rif cordilleras (Miocene to the present), *Tectonophysics*, *227*, 105 – 126, 1993.

Galindo-Zaldívar, J., A. Jabaloy, F. González-Lodeiro, and F. Aldaya, Crustal structure of the central sector of the Betic Cordillera (SE Spain), *Tectonics*, *16*, 18 – 37, 1997.

Galindo-Zaldívar, J., A. Jabaloy, I. Serrano, J. Morales, F. González-Lodeiro, and F. Torcal, Recent and present-day stresses in the Granada Basin (Betic Cordilleras): Example of a late Miocene-present-day extensional basin in a convergent plate boundary, *Tectonics*, *18*, 686 – 702, 1999.

Gans, P. B., E. L. Miller, J. McCarthy, and M. L. Ouldcott, Tertiary extensional faulting and evolving ductile-brittle transition zones in the northern Snake Range and vicinity: New insights from seismic data, *Geology*, *13*, 189 – 193, 1985.

García-Dueñas, V., and J. M. Martínez-Martínez, Sobre el adelgazamiento Mioceno del Dominio Cortical de Alborán: El despegue extensional de Filabres, *Geogaceta*, *5*, 53 – 55, 1988.

García-Dueñas, V., J. M. Martínez-Martínez, and F. Navarro-Vilá, La zona de falla de Torres Cartas, conjunto de fallas normales de bajo-ángulo entre Nevado-Filábres y Alpujárrides (Sierra de Alhamilla, Béticas Orientales), *Geogaceta*, *1*, 17 – 19, 1986.

García-Dueñas, V., J. M. Martínez-Martínez, M. Orozco, and J. I. Soto, Plis-nappes, cisaillements syn- à post-metamorphiques et cisaillements ductiles-fragiles en distension dans les Nevado-Filabrides (Cordillères Bétiques, Espagne), *C. R. Acad. Sci., Ser. II*, *307*, 1389 – 1395, 1988.

García-Dueñas, V., J. C. Balanyá, and J. M. Martínez-Martínez, Miocene extensional detachments in the outcropping basement of the northern Alborán basin (Betics) and their tectonic implications, *Geo Mar. Lett.*, *12*, 88 – 95, 1992.

García-Dueñas, V., E. Banda, M. Torné, D. Córdoba, and ESCI-Béticas Working Group, A deep seismic reflection survey across the Betic Chain (southern Spain): First results, *Tectonophysics*, *232*, 77 – 89, 1994.

García-García, F., C. Viseras, and J. Fernández, Organización secuencial de abanicos deltaicos controlados por la tectónica (Tortoniense superior, Cuenca de Granada, Cordillera Bética), *Rev. Soc. Geol. Esp.*, *12*, 199 – 208, 1999.

Getty, S. R., and L. P. Gromet, Evidence for extension at the Willimantic Dome, Connectiut: Implications for the late Paleozoic tectonic evolution of the New England Appalachians, *Am. J. Sci.*, *292*, 398 – 420, 1992.

Gibbs, A. D., Balanced cross-section construction from seismic sections in areas of extensional tectonics, *J. Struct. Geol.*, *5*, 153 – 160, 1983.

Goffé, B., et al., First evidence of high-pressure, low-temperature metamorphism in the Alpujarride nappes, Betic Cordillera (SE Spain), *Eur. J. Mineral.*, *1*, 139 – 142, 1989.

Gómez-Pugnaire, M. T., and J. M. Fernández-Soler, High-pressure metamorphism in metabasites from the Betic Cordilleras (SE Spain) and its evolution during the Alpine orogeny, *Contrib. Mineral. Petrol.*, *95*, 231 – 244, 1987.

González-Casado, J. M., C. Casquet, J. M. Martínez-Martínez, and V. García-Dueñas, Retrograde evolution of quartz segregations from the Dos Picos shear zone in the Nevado-Filabride Complex (Betic chains, Spain): Evidence from fluid inclusions and quartz c-axis fabrics, *Geol. Rundsch.*, *84*, 175 – 186, 1995.

Hamilton, W., Crustal extension in the Basin and Range Province, southwestern United States, in *Continental Extensional Tectonics*, edited by M. P. Coward, J. F. Dewey, and P. L. Hancock, *Geol. Soc. Spec. Publ.*, *28*, 155 – 176, 1987.

Hartz, E. H., and A. Andressen, From collision to collapse: Complex strain permutations in the hinterland of the Scandinavian Caledonides, *J. Geophys. Res.*, *102*, 24,697 – 24,711, 1997.

Herraiz, M., et al., The recent (upper Miocene to Quaternary) and present tectonic stress distributions in the Iberian Peninsula, *Tectonics*, *19*, 762 – 786, 2000.

Holt, W. E., C. G. Chase, and T. C. Wallace, Crustal structure from three-dimensional gravity modeling of a metamorphic core complex: A model for uplift, Santa Catalina-Rincon Mountains, Arizona, *Geology*, *14*, 827 – 830, 1986.

Howard, K. A., and D. A. Foster, Thermal and unroofing history of a thick, tilted Basin-and-Range crustal section in the Tortilla Mountains, Arizona, *J. Geophys. Res.*, *101*, 511 – 522, 1996.

Jabaloy, A., J. Galindo-Zaldívar, and F. González-Lodeiro, The Alpujarride-Nevado-Filabride extensional shear zone, Betic Cordilleras, SE Spain, *J. Struct. Geol.*, *15*, 555 – 569, 1993.

Jackson, M. P. A., and W. E. Galloway, Structural and depositional styles of Gulf Coast Tertiary continental margin: Application to hydrocarbon exploration, *AAPG Continuing Ed. Course Notes Ser.*, 226 pp., 1984.

Janecke, S. U., C. J. Vanderburg, and J. B. Blankenau, Geometry, mechanisms and significance of extensional folds from examples in the Rocky Mountain Basin and Range province, U.S.A., *J. Struct. Geol.*, *20*, 841 – 856, 1998.

John, B. E., Geometry and evolution of a mid-crustal extensional fault system: Chemehuevi Mountains, southeastern California, in *Continental Extensional Tectonics*, edited by M. P. Coward, J. F. Dewey, and P. L. Hancock, *Geol. Soc. Spec. Publ.*, *28*, 313 – 335, 1987.

John, B. E., and D. A. Foster, Structural and thermal constraints on the initiation angle of the detachment faulting in the southern Basin and Range: The Chemehuevi Mountains case study, *Geol. Soc. Am. Bull.*, *105*, 1091 – 1108, 1993.

John, B. E., and K. A. Howard, Rapid extension recorded by cooling-age patterns and brittle deformation, Naxos, Greece, *J. Geophys. Res.*, *100*, 9969 – 9979, 1995.

Johnson, C., Resolving denudational histories in orogenic belts with apatite fission-track thermochronology and structural data: An example from southern Spain, *Geology*, *25*, 623 – 625, 1997.

Johnson, C., N. Harbury, and A. J. Hurford, The role of extension in the Miocene denudation of the Nevado-Filábride Complex, Betic Cordillera (SE Spain), *Tectonics*, *16*, 189 – 204, 1997.

King, G., and M. Ellis, The origin of large local uplift in extensional regions, *Nature*, *348*, 689 – 692, 1990.

Kleverlaan, K., Neogene history of the Tabernas basin (SE Spain) and its Tortonian submarine fan development, *Geol. Mijnbouw*, *68*, 421 – 432, 1989.

Kruger, J. M., J. E. Faulds, S. J. Reynolds, D. A. Okaya, Seismic reflection evidence for detachment polarity beneath a major accommodation zone, west-central Arizona, in *Accommodation Zones and Transfer Zones: The Regional Segmentation of the Basin and Range Province*, edited by J. E. Faulds and J. H. Stewart, *Geol. Soc. Am. Spec. Pap.*, *323*, 89 – 113, 1998.

Kruse, S., M. McNutt, J. Phipps-Morgan, L. Royden, and B. Wernicke, Lithospheric extension near Lake Mead, Nevada: A model for ductile flow in the lower crust, *J. Geophys. Res.*, *96*, 4435 – 4456, 1991.

Kurz, W., and F. Neubauer, Deformation partitioning during updoming of the Sonnblick area in the Tauern Window (Eastern Alps, Austria), *J. Struct. Geol.*, *18*, 1327 – 1343, 1996.

Lammerer, B., and M. Weger, Footwall uplift in an orogenic wedge: The Tauern Window in the Eastern Alps of Europe, *Tectonophysics*, *285*, 213 – 230, 1998.

Langenberg, C. W., Gravitational gliding in the northern Sierra de los Filabres (SE Spain), *Geol. Mijnbouw*, *52*, 187 – 192, 1973.

Lavier, L. L., W. R. Buck, and A. N. B. Poliakov, Self-consistent rolling-hinge model for the evolution of large-offset normal faults, *Geology*, *27*, 1127 – 1130, 1999.

Lee, J., Rapid uplift and rotation of mylonitic rocks from beneath a detachment fault: Insights from potassium feldspar $^{40}Ar/^{39}Ar$ thermochronology, northern Snake Range, Nevada, *Tectonics*, *14*, 54 – 77, 1995.

Leine, L., On the tectonics of the Menas de Serón region, western Sierra de los Filabres, SE Spain, *Proc. K. Ned. Akad. Wet. Amsterdam*, *69*, 403 – 414, 1966.

Lonergan, L., and M. Mange-Rajetzky, Evidence for Internal Zone unroofing from foreland basin sediments, Betic Cordillera, SE Spain, *J. Geol. Soc. London*, *151*, 515 – 529, 1994.

Lonergan, L., and N. White, Origin of the Betic-Rif mountain belt, *Tectonics*, *16*, 504 – 522, 1997.

Lynch, H. D., and P. Morgan, The tensile strength of the lithosphere and the localisation of extension, in *Continental Extensional Tectonics*, edited by M. P. Coward, J. F. Dewey, and P. L. Hancock, *Geol. Soc. Spec. Publ.*, *28*, 53 – 65, 1987.

Mancktelow, N. S., and T. L. Pavlis, Fold-fault relationships in low-angle detachment systems, *Tectonics*, *13*, 668 – 685, 1994.

Manning, A. H., and J. M. Bartley, Postmylonitic deformation in the Raft River metamorphic core complex, northwestern Utah: Evidence of a rolling hinge, *Tectonics*, *13*, 596 – 612, 1994.

Martín, J. M., and J. C. Braga, Tectonic signals in the Messinian stratigraphy of the Sorbas Basin (Almería, SE Spain), in *Tertiary Basins of Spain: The Stratigraphic Record of Crustal Kinematics*, *World and Reg. Geol. Ser.*, vol. 6, edited by P. F. Friend and C. J. Dabrio, pp. 387 – 391, Cambridge Univ. Press, New York, 1996.

Martínez-Martínez, J. M., and J. M. Azañón, Mode of extensional tectonics in the southeastern Betics (SE Spain): Implications for the tectonic evolution of the peri-Alborán orogenic system, *Tectonics*, *16*, 205 – 225, 1997.

Martínez-Martínez, J. M., J. I. Soto, and J. C. Balanyá, Large scale structures in the Nevado-Filabride Complex and crustal seismic fabrics of the deep seismic reflection profile ESCI-Béticas 2, *Rev. Soc. Geol. Esp.*, *8*, 477 – 489, 1997a.

Martínez-Martínez, J. M., J. I. Soto, and J. C. Balanyá, Crustal decoupling and intracrustal flow beneath domal exhumed core complexes, Betics (SE Spain), *Terra Nova*, *9*, 223 – 227, 1997b.

Mazzoli, S., and M. Helman, Neogene patterns of relative plate motion for Africa-Europe: some implications for recent central Mediterranean tectonics, *Geol. Rundsc.*, *83*, 464 – 468, 1994.

Melosh, H. J., Mechanical basis for low-angle normal faulting in the Basin and Range province, *Nature*, *343*, 331 – 335, 1990.

Miller, J. M. G., and B. E. John, Sedimentations patterns support seismogenic low-angle normal faulting, southeastern California and western Arizona, *Geol. Soc. Am. Bull.*, *111*, 1350 – 1370, 1999.

Monié, P., J. Galindo-Zaldívar, F. González-Lodeiro, B. Goffé, and A. Jabaloy, $^{40}Ar/^{39}Ar$ geochronology of Alpine tectonism in the Betic Cordilleras (southern Spain), *J. Geol. Soc. London*, *148*, 289 – 297, 1991.

Morales, J., I. Serrano, F. Vidal, and F. Torcal, The depth of the earthquake activity in the central Betics (southern Spain), *Geophys. Res. Lett.*, *24*, 3289 – 3292, 1997.

Nijhuis, H. J., Plurifacial Alpine metamorphism in the south-eastern Sierra de los Filabres, south of Lubrín, SE Spain, Ph.D. thesis, 151 pp., Univ. of Amsterdam, Amsterdam, 1964.

Orozco, M., J. M. Molina, A. Crespo-Blanc, and F. M. Alonso-Chaves, Paleokarst and rauhwacke development, mountain uplift and subaerial sliding of tectonic sheets (northern Sierra de los Filabres, Betic Cordilleras, Spain), *Geol. Mijnbouw*, *78*, 103 – 117, 1999.

Ott D'Estevou, P., and C. Montenat, Le bassin de Sorbas-Tabernas, in *Les Bassins Neogenes du Domaine Bétique Oriental* (*Espagne*), edited by C. Montenat, *Doc. Trav. Inst. Geol. Albert-de-Lapparent, Paris*, *12 – 13*, 101 – 128, 1990.

Pascual, A. M., La cuenca Neógena de Tabernas (Cordilleras Béticas), Ph.D. thesis, University of Granada, Granada, Spain, 1997.

Platt, J. P., and R. L. M. Vissers, Extensional collapse of thickened continental lithosphere: A working hypothesis for the Alborán Sea and Gibraltar Arc, *Geology*, *17*, 540 – 543, 1989.

Platt, J. P., B. Van der Eeckhout, E. Janzen, G. Konert, O. J. Simon, and R. Weijermars, The structure and tectonic evolution of the Aguilón nappe, Sierra Alhamilla, Betic Cordilleras, SE Spain, *J. Struct. Geol.*, *5*, 519 – 535, 1983.

Platt, J. P., J. H. Behrmann, J. M. Martínez-Martínez, and R. L. M. Vissers, A zone of mylonite and related ductile deformation beneath the Alpujarride nappe complex, Betic Cordilleras, S Spain, *Geol. Rundsch.*, *73*, 773 – 785, 1984.

Ranalli, G., *Rheology of the Earth: Deformation and Flow Processes in Geophysics and Geodynamics*, 366 pp., Allen and Unwin, Concord, Mass., 1987.

Rehrig, W. A., and S. J. Reynolds, Geologic and geochronologic reconnaissance of a northwest-trending zone of metamorphic core complexes in southern and western Arizona, in *Cordilleran Metamorphic Core Complexes*, edited by M. D. J. Critteden, P. J. Coney, and G. H. Davis, *Mem. Geol. Soc. Am.*, *153*, 131 – 157, 1980.

Reynolds, S. J., and G. S. Lister, Folding of mylonitic zones in Cordilleran metamorphic core complexes: evidence from near the mylonitic front, *Geology*, *18*, 216 – 219, 1990.

Rodríguez-Fernández, J., and C. Sanz de Galdeano, Onshore Neogene stratigraphy in the north of the Alborán Sea (Betic Internal Zones): paleogeographic implications, *Geo Mar. Lett.*, *12*, 123 – 128, 1992.

Rodríguez-Fernández, J., M. C. Comas, J. Soria, J. A. Martín-Pérez, and J. I. Soto, The sedimentary record of the Alborán Basin: An attempt at sedimentary sequence correlation and subsidence analysis, *Proc. Ocean Drill. Program. Sci. Results*, *161*, 69 – 76, 1999.

Royden, L. H., The tectonic expression of slab pull at continental convergent boundaries, *Tectonics*, *12*, 303 – 325, 1993.

Sanz de Galdeano, C., J. Rodríguez-Fernández, and A. C. López-Garrido, A strike-slip fault corridor within the Alpujarra Mountains (Betic Cordilleras, Spain), *Geol. Rundsch.*, *74*, 641 – 655, 1985.

Selverstone, J., G. J. Axen, and J. M. Bartley, Fluid inclusion constraints on the kinematics of footwall uplift beneath the Brenner Line normal fault, eastern Alps, *Tectonics*, *14*, 264 – 278, 1995.

Serrano, I., J. Morales, F. Vidal, and F. Torcal, Mecanismos focales en la cuenca de Granada, in *Libro Homenaje a Fernando de Miguel Martinez*, edited by F. Vidal and M. Espinar, pp. 619 – 640, Serv. de Publ. de la Univ. de Granada, Granada, 1996.

Sonder, L. J., P. C. England, B. P. Wernicke, and R. L. Christiansen, A physical model for Cenozoic extension of western North America, in *Continental Extensional Tectonics*, edited by M. P. Coward, J. F. Dewey, and P. L. Hancock, *Geol. Soc. Spec. Publ.*, *28*, 187 – 201, 1987.

Soria, J. M., C. Viseras, and J. Fernández, Late Miocene-Pleistocene tectono-sedimentary evolution and subsidence history of the central Betic Cordillera (Spain): A case study in the Guadix intramontane basin, *Geol. Mag.*, *135*, 565 – 574, 1998.

Soto, J. I., Estructura y evolución metamórfica del complejo Nevado-Filábride en la terminación oriental de la Sierra de los Filabres (Cordilleras Béticas), Ph.D. thesis, 274 pp., Univ. of Granada, Granada, Spain, 1991.

Soto, J. I., V. García-Dueñas, and J. M. Martínez-Martínez, El valor de la deformación dúctil asimétrica en el ortogneis de Lubrín, Almería (Manto de Bédar-Macael, Complejo Nevado-Filábride), *Geogaceta*, *7*, 92 – 94, 1990.

Spencer, J. E., The role of tectonic denudation in the warping and uplift of low-angle normal faults, *Geology*, *12*, 95 – 98, 1984.

Spencer, J. E., Miocene low-angle normal faulting and dike formation, Homer Mountains and surrounding areas, southeastern California, *Geol. Soc. Am. Bull.*, *96*, 1140 – 1155, 1985.

Spencer, J. E., and S. J. Reynolds, Tectonics of mid-Tertiary extension along a transect through west central Arizona, *Tectonics*, *10*, 1204 – 1221, 1991.

Stapel, G., R. Moeys, and C. Biermann, Neogene evolution of the Sorbas basin (SE Spain) determined by paleostress analysis, *Tectonophysics*, *255*, 291 – 305, 1996.

Stüwe, K., and T. D. Barr, On the relationship between surface uplift and gravitational extension, *Tectonics*, *19*, 1056 – 1064, 2000.

Suppe, J., Geometry and kinematics of fault bend folding, *Am. J. Sci.*, *283*, 684 – 721, 1983.

Tari, G., P. Dövényi, I. Dunkl, F. Horváth, L. Lenkey, M. Stefanesku, P. Szafián, and T. Tóth, Lithospheric structure of the Pannonian basin derived from seismic, gravity and geothermal data, in *The Mediterranean Basins: Tertiary Extension Within the Alpine Orogen*, edited by B. Durand, et al., *Geol. Soc. Spec. Publ.*, *156*, 215 – 250, 1999.

Torné, M., M. Fernàndez, M. C. Comas, and J. I. Soto, Lithospheric structure beneath the Alborán Basin: Results from 3D gravity modeling and tectonic relevance, *J. Geophys. Res.*, *105*, 3209 – 3228, 2000.

Tubía, J. M., J. Cuevas, F. Navarro-Vilá, F. Alvarez, and F. Aldaya, Tectonic evolution of the Alpujarride Complex (Betic Cordillera, southern Spain), *J. Struct. Geol.*, *14*, 193 – 203, 1992.

Verrall, P., Structural interpretation with application to North Sea problems, *Joint Assoc. for Petrol. Explor. Courses Course Notes*, *3*, Petrol. Explor. Soc. of Great Britain, London, 1981.

Voet, H. W., Evidence of "late" alpine overthrusting, in the region NW of Líjar, Sierra de los Filabres (SE Spain), *Geol. Mijnbouw*, *43*, 10 – 12, 1964.

Wdowinski, S., and G. J. Axen, Isostatic rebound due to tectonic denudation: A viscous flow model of a layered lithosphere, *Tectonics*, *11*, 303 – 315, 1992.

Weijermars, R., T. D. Root, B. Van der Eeckhout, R. Postma, and K. Kleverlaan, Uplift history of a Betic fold nappe inferred from Neogene-Quaternary sedimentation and tectonics (in the Sierra Alhamilla and Almeria, Sorbas and Tabernas Basins of the Betic Cordilleras, SE Spain), *Geol. Mijnbouw*, *64*, 397 – 411, 1985.

Weissel, J. K., and G. D. Karner, Flexural uplift of rift flanks due to mechanical unloading of the lithosphere during extension, *J. Geophys. Res.*, *94*, 13,919 – 13,950, 1989.

Wernicke, B., The fluid crustal layer and its implications for continental dynamics, in *Exposed Cross-Sections of the Continental Crust*, edited by M. H. Salisbury and D. M. Fountain, pp. 509 – 544, Kluwer Acad., Norwell, Mass., 1990.

Wernicke, B., Cenozoic extensional tectonics of the U.S. Cordillera, in *The Geology of North America*, vol. G3, *The Cordilleran Orogen: Conterminous U.S.*, edited by B. C. Burchfiel, P. W. Lipman, and M. L. Zoback, pp. 553 – 581, Geol. Soc. of Am., Boulder, Colo., 1992.

Wernicke, B., and G. J. Axen, On the role of isostasy in the evolution of normal fault systems, *Geology*, *16*, 848 – 851, 1988.

White, N. J., J. A. Jackson, and D. P. McKenzie, The relationship between the geometry of normal faults and that of sedimentary layers in their hanging walls, *J. Struct. Geol.*, *8*, 897 – 909, 1986.

Wildi, W., La Chaine tello-rifaine (Algérie, Maroc, Tunisie): Structure, stratigraphie et évolution du Trias au Miocène, *Rev. Géogr. Phys. Géol. Dyn.*, *24*, 201 – 297, 1983.

Yin, A., Origin of regional, rooted low-angle normal faults: A mechanical model and its tectonic implications, *Tectonics*, *8*, 469 – 482, 1989.

Yin, A., Mechanisms for the formation of domal and basinal detachment faults: A three-dimensional analysis, *J. Geophys. Res.*, *96*, 14,577 – 14,594, 1991.

Yin, A., and J. F. Dunn, Structural and stratigraphic development of the Whipple-Chemehuevi detachment fault system, southeastern California: Implications for the geometrical evolution of domal and basinal low-angle normal faults, *Geol. Soc. Am. Bull.*, *104*, 659 – 674, 1992.

Yin, A., T. M. Harrison, M. A. Murphy, M. Grove, S. Nie, F. J. Ryerson, W. X. Feng, and C. Z. Le, Tertiary deformation history of southeastern and southwestern Tibet during the Indo-Asian collision, *Geol. Soc. Am. Bull.*, *111*, 1644 – 1664, 1999.

J. C. Balanyá, Departamento de Ciencias Ambientales, Facultad de Ciencias Experimentales, Universidad Pablo de Olavide, Sevilla, Sevilla, Spain. (jcbalrou@dex.upo.es)

J. M. Martínez-Martínez and J. I. Soto, Instituto Andaluz de Ciencias de la Tierra (CSIC) and Departamento de Geodinámica, Universidad de Granada, Av. Fuentenueva s/n, 18071 Granada, Spain. (jmmm@ugr.es; jsoto@ugr.es)